FE-2030-6

CHARACTERISTICS OF AMERICAN COALS IN RELATION TO THEIR CONVERSION INTO CLEAN ENERGY FUELS

Quarterly Technical Progress Report, October—December 1976

W. Spackman
A. Davis
P. L. Walker
H. L. Lovell
R. H. Essenhigh
F. J. Vastola
P. H. Given

March 1977

Work Performed Under Contract No. EX-76-C-01-2030

Coal Research Section
Pennsylvania State University
University Park, Pennsylvania

ENERGY RESEARCH AND DEVELOPMENT ADMINISTRATION

DISCLAIMER

NOTICE

Available from the National Technical Information Service, U. S. Department of Commerce, Springfield, Virginia 22161

Price: Paper Copy $4.50 (domestic)
$7.00 (foreign)
Microfiche $3.00 (domestic)
$4.50 (foreign)

FE-2030-6
Distribution Categories UC-90a, b, c, d and f

THE CHARACTERISTICS OF AMERICAN COALS IN RELATION TO THEIR CONVERSION INTO CLEAN ENERGY FUELS

Quarterly Technical Progress Report
October - December 1976

by
W. Spackman, A. Davis, P.L. Walker, H.L. Lovell,
R.H. Essenhigh, F.J. Vastola and P.H. Given

COAL RESEARCH SECTION
THE PENNSYLVANIA STATE UNIVERSITY
UNIVERSITY PARK, PENNSYLVANIA 16802

ABSTRACT

Under Facet I, 49 coal samples have been added to the Penn State/ ERDA Sample Bank. Sixty-six characterized coal samples and 734 sets of analytical data were provided upon request to other agencies.

Facet IV-A research on reactor development and operation has led to the construction of a cold model for the flow of gases through the combustion pot. Flow analyses indicate that even with relatively slow flows the mainstream flow is turbulent.

Methanol and water densities of a series of char samples, studied under Facet IV-B, were found to be quite similar. Deposition of carbon on chars from the cracking of methane results in a reduction of char surface area and open pore volume.

Siderite and calcite catalyze the cracking of methane at 900°C. No catalytic activity is evidenced for dolomite, pyrite, illite, quartz, rutile, or kaolinite in this reaction.

From a comparison of refractory and water-cooled bottom blocks, under Facet V-A, it was found that even significant changes in the furnace bottom temperature can only cause moderate changes in plane-flame furnace combustion performance.

TABLE OF CONTENTS

	Page
ABSTRACT	i
OBJECTIVE AND SCOPE OF WORK	iv
TASK DESCRIPTIONS	v
SUMMARY OF PROGRESS TO DATE	1
SAMPLE COLLECTION AND SEAM CHARACTERIZATION	3
Coal Sampling	3
Sampling Survey	3
COAL CHARACTERIZATION	4
Coal Characterization	4
Rapid Scan Automated Reflectance Microscope System	4
Hot-Stage Microscopy	5
SAMPLE BANK OPERATION, MAINTENANCE, AND DEVELOPMENT	6
Service to Other Agencies	6
PENN STATE/ERDA COAL DATA BASE	7
Coal Data Base Activity Report	7
COAL BENEFICIATION AND PRE-USE PROCESSING	8
Coal Preparation Studies	8
REACTOR DEVELOPMENT AND OPERATION	11
Evaluation of the Gasification Potential of Coals	11
Effect of Heating Rate and Soak Temperature on Volatile Matter Release	12
Characteristics of Chars Produced by Pyrolysis Following Rapid Heating of Pulverized Coal	16
COKES AND CHARS	22
Methanol and Water Densities of Coal Chars	22
Effect of Carbon Deposition on the Porosity and Reactivity of Air	25
Chemisorption of Oxygen on Carbonaceous Solids	32
Catalytic Activity of Minerals for the Cracking of Methane	38
Reactivity of Ion-Exchanged Lignite Chars in Steam	44
COMBUSTION OF CHARS AND LOW VOLATILE FUELS	46
Combustion of Char and Anthracite Coal in Large Utility Boilers	46
COMBUSTION OF COAL-OIL EMULSTIONS	56
Combustion of Coal-Oil-Water Mixture	56
CONCLUSIONS	57

Page

REFERENCES 59

CONTRIBUTORS 61

OBJECTIVE AND SCOPE OF WORK

The primary objective of the overall program is to achieve the capability of predicting, from a knowledge of coal composition, the behavior of a coal in pre-conversion processing, coal gasification and coal liquefaction processes.

It is reasonable to ask if this goal is in fact attainable, recognizing the heterogeneity of coal seams. Clearly, it is not if one concerns oneself simply with the rank of the coal seam and its aggregate chemistry. A high volatile B coal from Indiana need not react to processing in the same manner as a high volatile B coal from Utah, even though their "chemistries" may be very similar. In contrast, a coal lithotype of a specific kind, at a given level of rank, can be expected to behave consistently, whether it derives from Alabama or Pennsylvania. Hence, the goal may very well be attainable if, as in the case of coal carbonization, we concern ourselves with the reacting entities and the properties of the important lithotypes.

The goal is to attain the same high level of predictive accuracy that is now found in the area of coal carbonization, where Penn State's collaborative work with the steel industry proved highly successful. To achieve this goal Penn State has devised an integrated program in which the success of the research is highly dependent on the effective operation of ALL of the program's Facets and Sub-facets which are as follows:

Facet I: Characterization of the Nation's Coal Resources
- I-A: Sample Collection and Seam Characterization
- I-B: Coal Characterization
- I-C: Sample Bank Operation, Maintenance and Development
- I-D: Penn State-ERDA Coal Data Base

Facet II: Coal Beneficiation and Pre-Use Processing

Facet IV: Significance of Coal Characteristics in Gasification Processes
- IV-A: Reactor Development and Operation
- IV-B: Cokes and Chars
- IV-D: Reactivity of Coal Chars
- IV-E: Catalysis Research
- IV-F: Differential Scanning Calorimetry

Facet V: Coal Combustion Research
- V-A: Combustion of Chars and Low Volatile Fuels
- V-B: Combustion of Coal-Oil Emulsions

THE CHARACTERISTICS OF AMERICAN COALS IN RELATION TO THEIR CONVERSION INTO CLEAN ENERGY FUELS

TASK DESCRIPTIONS

FACET I-A	Sample Collection and Seam Characterization
Task 1	Sampling Survey
Task 2	Sampling Plan
Task 3	Sampling
FACET I-B	Coal Characterization
Task 5	Characteristics and Use Potential of U. S. Coal Seams
Task 6	Characterization of Other ERDA Contractor Samples
Task 7	Automation of Microscopic Analytical Methods
FACET I-C	Sample Bank Operation, Maintenance and Development
Task 8	Maintenance of Coal Sample Bank
Tasks 9-14	Provision of Samples and Data to Penn State and Other Investigators
FACET I-D	Penn State/ERDA Coal Data Base
Task 15	Computerization of Data
Task 16	Evaluation of the Data Base
Task 17	Structuring and Utilization of the Data Base
FACET II	Coal Beneficiation and Pre-Use Processing
Task 18	Washability Characterization
Task 19	Physical Properties of Coal Lithotypes
Task 20	Techniques for Fractionation
Task 21	Beneficiation of Conversion Feedstocks
Task 22	Evaluation of Dry Flo Separator
FACET IV-A	Reactor Development and Operation
Task 23	Operation of Isothermal Furnace
Task 24	Pyrolysis of Coal Lithotypes
Task 25	Operation of Pressurized Isothermal Reactor
Task 26	Coal Reactivity
FACET IV-B	Cokes and Chars
Task 27	Effect of Variables on Char Structures
Task 28	Effect of Char Structures on Reactivities
Task 29	Catalytic Effect of Minerals in Gasification
Task 30	Effect of Catalytic Cations on Gasification
FACET IV-F	Differential Scanning Calorimetry
Task 31	DSC in Evaluating Coals for Conversion
FACET V-A	Combustion of Chars and Low Volatile Fuels
Task 32	Flame Ball Combustion Model
Task 33	Plane Flame Furnace
FACET V-B	Combustion of Coal - Oil Emulsions
Task 34	Combustion of Coal - Oil Emulsions

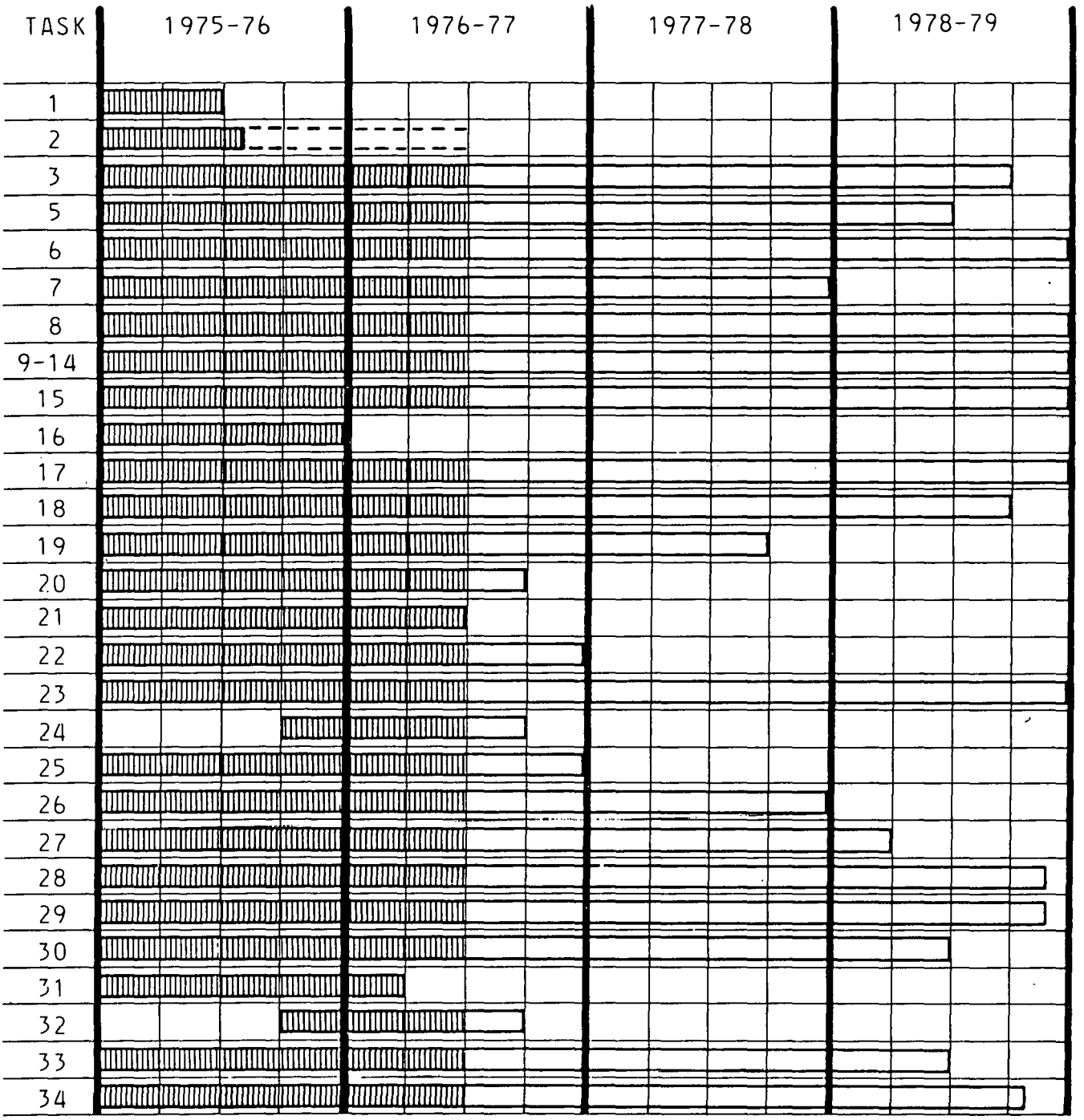

LEGEND

SCHEDULED

PROGRESS

SCHEDULE EXTENSION

EARLY START

PROJECT PLAN AND PROGRESS REPORT

Quarter Ending December 31, 1976

SUMMARY OF PROGRESS TO DATE

Forty-nine additional coal samples were added to the Penn State/ERDA Coal Sample Bank during the report period. Sixty-six characterized coal samples and 734 sets of analytical data were provided upon request to other agencies engaged in coal research.

Research on the Rapid Scan has recently been directed toward the characterization of the pyritic sulfur content in coals. Work continues in refining Rapid Scan analyses of vitrinite reflectance.

Under Facet II, to date thirteen samples of twelve seams, representing six ranks, have been fractionated for washability characterization. Studies are underway investigating conversion potential of a low calorific value Texas coal (PSOC-575 through 579), using coal beneficiation to produce adequate sulfur rejection.

Construction of the pressurized laminar-flow isothermal reactor of Facet IV-A continues, with delivery expected by March or April, 1977. Preliminary plans for an appropriate building facility to house the reactor have been prepared and are being considered by the University.

Results of the study on mechanisms of gasification in a combustion pot have been presented in a previous report. This work has continued with a digression to coal model flow measurements of pressure drop through a fuel bed for various particle sizes and flow rates. Although low rates usually indicate laminar flow, the coal flow measurements indicate that the mainstream flow in the bed is turbulent.

To complement further experimental studies of the combustion pot, preliminary work has been started on a predictive model which considers chemical kinetics, variation of porosity, heat and mass transfer, and the effect of pressure gradient through the bed.

The rapid heating (of the order of 8×10^3°C/sec) of a North Dakota lignite (PSOC-246) in a nitrogen atmosphere has been studied using a laminar flow isothermal furnace. The effect of residence times up to about 1 sec at maximum temperature (808°C) on changes in coal properties and weight loss has been studied. For residence times up to about 1 sec the lignite is found to undergo a monotonic decrease in weight and a monotonic increase in surface area and density. Changes which the coal undergoes during the heating period are negligible compared to changes produced while at maximum temperature.

Methanol and water density studies have been conducted on lignite char under Facet IV-B. A series of thirteen samples were prepared from a lignite char by 1) depositing different amounts of carbon by the cracking of methane and 2) activation of the raw and carbon deposited samples to different levels of carbon burn-off. Methanol and helium densities were found to be close.

Carbon deposition from the cracking of methane into the pores of a lignite char has been studied. Carbon deposition occurs at a significant

rate at temperatures between 815 and 855°C. Removal of the inorganic impurities from the char by acid-washing significantly reduces the extent of carbon deposition.

Differential scanning calorimetry has been established as a fast experimental technique for characterization of carbonaceous materials. The effect of different variables such as the level of burn-off, particle size, and bed height of the carbon, as well as reaction temperature and flow rate on the heat of chemisorption of oxygen on Saran carbons has been examined. The existence of different kinetic stages corresponding to adsorption on different active sites is indicated. The rate of heat released during chemisorption is proportional to the square root of oxygen partial pressure. Heat of chemisorption of oxygen on a Saran carbon containing 101 ppm iron as an impurity has been found to be 65 kcal/mole.

The catalytic activity of major minerals is being investigated for the first time under this contract as it applies to the cracking of methane.

A variety of cations are being systematically examined to establish their roles in determining the rates of the steam/char reaction for a heat treated lignite.

Computer models are being analyzed to study the combustion of pulverized char flames under Facet V-A assuming an infinite parallel plane geometry (properties varying only along direction of flow), a logical and valid starting point toward further three dimensional modeling. Modification to the model such as uneven nodal spacing, variable radiation absorption coefficient, and diffusional limitations on combustion rates have brought the results of the model closer to experimental reality. The effect of varying parameters such as combustor length (between walls) and fuel reactivity has been investigated. A study was also performed to compare the operations of the plane-flame furnace with a refractory bottom (as usual) and with a water-cooled metal bottom. Four coal chars have been burned in the plane-flame furnace at common air flow rates.

The combustion characteristics of coal-oil-water mixtures are being studied under Facet V-B using a hot-wall furnace. The effect of trace additives of coal, and of percent additions up to over 7 percent of coal, on the heat transfer and combustion characteristics of water-oil-air mixtures have been studied. The coal additions increase heat output from the furnace to levels higher than those of fuel oil alone, without significant changes in excess air requirements for complete combustion, whereas levels of soot emissions are comparable to that of fuel oil alone. Separate tests have revealed a changing histeresis effect in the thermal output of the furnace as a function of firing rate, suggesting that adequate preheat periods should be provided before subsequent test runs. Over one hundred and thirty experiments have been performed so far in the execution of this research.

FACET I-A: SAMPLE COLLECTION AND SEAM CHARACTERIZATION

COAL SAMPLING

Although no sampling trips were made by Penn State personnel during this period, many samples were received from other agencies. Twenty-nine samples from six different sites were sent by Southern Illinois University; fourteen samples were shipped to us by the University of Utah and six cores, with at least sixteen coal seams included, were received from the Denver office of the United States Geological Survey.

SAMPLING SURVEY

A nationwide survey to determine the extent to which the Nation's coal seams have been sampled and characterized has been completed. A report of these findings is in preparation.

FACET I-B: COAL CHARACTERIZATION

COAL CHARACTERIZATION

During this period, maceral analyses were completed on two samples supplied by other ERDA contractors (POC-290 and 291) and 20 PSOC samples (PSOC-392 through 411). Reflectance analyses were completed on 12 new samples (PSOC-394 and PSOC-410 through 420) while five older samples were redone for vitrinite and pseudovitrinite reflectance and 23 older samples were analyzed for pseudovitrinite reflectance. An ultraviolet light maceral analysis was performed on PSOC-394. In addition, FSI analyses were run on 110 coals, Gray-King Coking tests on 43 samples, and Hardgrove Grindability on 78 samples. Polished blocks for Vickers Microhardness tests were prepared for 25 coals, 130 new samples were split out and delivered, along with 25 splits of coals previously supplied, to the Mineral Constitution Laboratories for elemental and mineralogic analyses. During this period, 21 samples were sent out for standard chemical analyses (PSOC-461-465, 467-470, 472, 474-476, 479-483, 485-486, and 394).

RAPID SCAN AUTOMATED REFLECTANCE MICROSCOPE SYSTEM

Research on the Rapid Scan system has been directed toward the characterization of the pyritic sulfur content in coals. Different techniques, such as point counting and lineal analysis are being examined and their precisions compared. Assumptions relating to the randomness of particles in a sample are being tested for validity so that biases in the Rapid Scan subsampling can be avoided. Another important aspect of the pyritic sulfur analysis is the rapid acquisition of size data, known as a random chord size distribution. By comparing the distributions from several coals, statistical inferences may be possible, but more research into the theoretical aspects of sampling and the size distributions is necessary. Ultimately, information concerning the relationship between pyrite chord size and the comminution of coal at the preparation plant will be valuable as an indication of proper sizing for maximum cleaning efficiency.

Work has also been involved with further improvements on the correction factor, which changes mean-average random vitrinite reflectance (MARR), to mean-maximum vitrinite reflectance. The Rapid Scan can now be used to predict mean-maximum reflectance with a precision of ± .06 percent R_0 (coals greater than 65% vitrinite). A series of samples were also analyzed to determine if the Rapid Scan could be used to measure reflectance of dispersed organic material. These samples indicate, that when the concentration of organic particles is high, the results are acceptable.

The reflectogram has been studied to determine how its resolution can be improved. It is believed that both improvements to equipment and programming will be necessary to increase resolution. Further work will be involved with improving the resolution, and relating the improved reflectogram to coal characterization techniques.

HOT-STAGE MICROSCOPY

Work on the hot-stage microscope system has been involved with mounting and testing the new Leitz 1350 heating stage on the current microscope facilities. Work has also begun on evaluating instrumental systems capable of controlling the system's heating rate. Future work will involve standardizing the new facility and evaluating the controller systems.

SERVICE TO OTHER AGENCIES

The coal research community has increasingly relied on the Penn State sample bank as a source of well characterized coal samples. During this report period 66 such samples and 734 selected printouts of coal data were supplied to other agencies.

Five samples were supplied to Adelphi University, and seven samples were sent to the General Electric Space Technology Center. The University of Southern California was sent three samples, the City College of the City University of New York received four samples, while two samples were sent to the Chemical Engineering Department of the California Institute of Technology. The Syracuse Research Institute requested and was sent seventeen samples, most of which were 50 to 100 pounds each. Two samples were supplied to the Chemistry Department of Penn State, four samples to the Chemical Engineering Department at Columbia University, and an additional two samples went to the Chemical Engineering Department at the University of Pennsylvania. The Gulf Research and Development Company was provided with sixteen small samples and the Rochester and Pittsburgh Coal Company received four samples prepared for use in microscopy.

FACET I-D: PENN STATE/ERDA COAL DATA BASE

COAL DATA BASE ACTIVITY REPORT

Work is underway to examine the interrelationships of select properties of U.S. channel samples as represented in the Penn State/ERDA Coal Data Base. The goal of this study is to obtain a better understanding of the interrelationships of commonly reported properties of coals and, as a result, to refine the use of specific properties for predicting technological behaviors of coal.

The properties being considered for all channel samples are moisture, volatile matter, calorific value, reflectance, petrographic components (percent vitrinite, exinite, and inertinite), and components of the ultimate analysis on a dry, mineral-free basis (carbon, hydrogen, oxygen, nitrogen and organic sulfur). The interrelations between these properties are being determined for the entire range of rank, excluding anthracites, and for several subgroups based on rank and province. Other subgroups, based on availability of data, are being examined to study free-swelling index, hardness, grindability, and Gray-King coke type and their relationships with the previously mentioned properties. Computerized statistical programs are being employed, such as the Penn State Statistical Package (a series of statistical programs developed by the Penn State Computer Center) and "CORFAN", a program compiled and developed by Ondrick and Srivastava[1] for correlations and factor analyses. Graphs and equations are being developed to present significant correlation between properties. All computer work is being done on the Penn State IBM 370/168 computer.

FACET II: COAL BENEFICIATION AND PRE-USE PROCESSING

COAL PREPARATION STUDIES

The petrographic analysis of PSOC-317 (a low volatile bituminous coal from the Lower Freeport seam in Pennsylvania) has been received and incorporated into the coal preparation data bank. This coal contained no exinite in the feed and none was detected in the gravity fractions. The analysis of the several fractions, in comparison with the head sample, were:

	Volume %	
	Range	Feed
Vitrinite	93.4-70.6	65.0
Micrinite	16.9- 4.9	22.8
Fusinite	12.5- 1.4	12.2

The studies of Task 18 involve the samples described in Table 1. The basic preparation characteristics of those samples whose fractionation has been recently completed are summarized in Table 2. To date, thirteen samples of twelve different seams, representing six ranks, have been fractionated. Currently, studies are proceeding on PSOC-242, another subbituminous B coal, from Wyoming. These completed studies represent more than 40 percent of the coals to be fractionated which represent six of the ten ranks to be studied. Additional ranks and coals to be considered include anthracite, medium volatile, high volatile B (Illinois) and subbitumionus A and C.

Further maceral concentration efforts have been made on PSOC-296 to 297, different portions of the exinite-rich Ohio No. 5 - Lower Kittanning seam (cannel coal).[2] The additional fractions from PSOC-297 (Hardnesses A and C, 3/8 in. x 1/4 in., 1.35 float) which contained 69.8 and 74.4 percent vitrinite, respectively (from a head sample containing 39.8 percent vitrinite) were combined and subject to additional liberation by stage crushing to minus 16 mesh and further separated at a density of 1.33 to attain a higher vitrinite content. The micrinite-fusinite concentrates in PSOC-296 to 297 (Hardnesses A and C, 3/8 in. x 1/4 in., 1.40 x 1.60) were also combined and further liberated at 16 mesh and separated at 1.50.

Fractionation studies were completed on an unusually high fusinite Australian coal (PSMC-10, ATHOL) seeking further fusinite concentration (Table 3). Since the available sample material had already been crushed to minus 20 mesh for petrographic analysis, it was sized at 60 and 200 mesh. Gravity fractions were developed utilizing centrifugal forces at 1.50 and 1.80 densities.

The interpretation of these data must involve due consideration of the distribution of the mineral matter since the maceral analyses are reported on a mineral matter-free basis. Obviously, it is possible to attain fusinite concentrates in excess of 80 percent.

Studies are underway on a low calorific content Texas coal (Eagle Pass, PSOC-575 through 579) utilizing portions of 3 in. cores from two seams (A and B). In addition to maceral concentrations, special consideration will be

Table 1. Identification of Coals Fractionated

PSOC No.	Rank	Paar Volatile Matter, %	Seam-Location
326	High Volatile A	43.8	Upper Kittanning Pennsylvania
337	High Volatile A	37.1	Lower Kittanning Pennsylvania
184	High Volatile C	42.0	Upper and Lower Banner Indiana
329	High Volatile A	42.6	Brookville Pennsylvania
317	Low Volatile	17.7	Lower Freeport Pennsylvania
183	High Volatile B	42.4	Upper Block Indiana
349	High Volatile A	42.5	Lower Clarion Pennsylvania
357	High Volatile A	34.3	Lower Elkhorn Kentucky
296	High Volatile A	43.1	Ohio No. 5-Lower Kittanning Ohio
297	High Volatile A	45.7	Ohio No. 5-Lower Kittanning Ohio
379	Semi-Anthracite	9.0	B Seam-Sullivan County Pennsylvania
383	Semi-Anthracite	10.6	A Seam-Sullivan County Pennsylvania
241	Subbituminous B	43.5	Monarch Seam Wyoming
242	Subbituminous B	46.0	Deitz Seam Wyoming

Table 2. Summary of Preparation Characteristics of Coals Recently Fractionated (dry basis)

Sample Designation	Feed	Clean Coal Product		
		Lowest Fraction	at 1.40 g/cc (+16 mesh)	at 1.80 g/cc (+16 mesh)
PSOC-383				
Ash, %	20.96	5.14	5.69	13.84
Sulfur, %	0.94	0.68	0.82	.82
Yield, %			14.9	74.5
Hardgrove Grindability Index				
A			62.2	
B			60.8	
C			59.4	

Table 2 (continued)

PSOC-241				
Ash, %	4.70	3.19	3.73	3.93
Sulfur, %	0.50	0.35	0.39	.41
Yield, %			79.7	84.0
Hardgrove Grindability Index				
A			56.7	
B			47.7	
C			44.9	

Table 3. Weight Distributions and Fractional Analyses: PSMC-10

Size Fraction	Weight, %	Volume % (mmf)			
		Vitrinite	Exinite	Micrinite	Fusinite
Head		35.9	0.0	5.4	58.7
20 x 60M	53.8				
1.50 Float	48.1	24.6	0.6	3.0	71.8
1.50 x 1.80	5.4	31.2	0.7	5.0	63.1
1.80 Sink	0.3	28.2	0.3	2.3	69.2
60 x 200M	24.0				
1.50 Float	21.0	24.3	0.9	2.5	72.3
1.50 x 1.80	2.7	17.0	0.5	2.9	83.6
1.80 Sink	0.3	31.6	1.3	3.7	63.4
Minus 200M	22.2				
1.50 Float	19.5	25.0	0.4	4.0	70.6
1.50 x 1.80	1.5	24.1	0.2	4.5	71.2
1.80 Sink	1.2	12.2	0.6	5.1	82.1

given to sulfur reduction and the presence of finely divided clays which result in high ash content and can create difficulties in any aqueous beneficiation process. In addition to potential conversion application, this coal may be utilized for steam generation purposes. In the latter situation, beneficiation potential would require high calorific recoveries as well as adequate sulfur rejection.

EVALUATION OF THE GASIFICATION POTENTIAL OF COALS

Introduction

Construction of the pressurized laminar-flow isothermal reactor continues with delivery expected by March or April, 1977. Preliminary plans for an appropriate building facility to house the reactor have been prepared. In simulation of the combustion pot, cold flow experiments in the fuel bed have been carried out to study the pressure drop through the bed as a function of flow rate and particle size.

Experimental

The study of pressure drop in the fuel bed, which maintains the flow of the reactants and the products through the bed, is as important as the chemical reactions. The cause of the pressure drop in large scale gasification reactors is difficult to determine even on a gross or overall basis because of the varying conditions of temperature, gas composition, fuel particle size, and ash deposit. The hot-flow systems can be represented by cold flow measurements and semi-empirical equations.

When a fluid is passed through a fixed bed of solids, there exists a pressure drop, ΔP, per unit length of the fuel bed, L. The pressure drop is proportional to the rate of the fluid flow, fluid viscosity, density, size, shape, and packing of the solid particles. At low flow rates or low modified Reynolds number based on the particle size, $D_p U_s \rho/\mu$, the pressure loss is due to various forces in laminar flow. A generally accepted equation for pressure drop per unit length is due to Carman[3]

$$-\frac{dP}{dL} = \frac{\Delta P}{L} = \frac{c}{g_c \phi^2} \frac{(1-\varepsilon)^2}{\varepsilon^3} \frac{\mu \bar{u}_s}{D_p^2} \qquad (1)$$

where c = constant = 180, $\frac{dP}{dL}$ = pressure gradient, ε = fractional void volume or bed voidage, μ = fluid viscosity, $\bar{u}_s$ = mean superficial velocity, ϕ is the shape factor for non-spherical particles on the ratio of the specific surface of spheres to the specific surface of particles, and D_p = particle diameter. This equation is valid for the viscous flow range $\phi D_p \bar{U}_s \rho/\mu(1-\varepsilon) < 20$.

At high flow rates corresponding to fully developed turbulent flow the energy distribution is directly proportional to the inertial forces or to the product of fluid density and square of the flow velocity. Carman[3] gives a relationship for $\frac{\phi D_p \bar{U}_s}{(1-\varepsilon)} > 100$ for the turbulent flow,

$$-\frac{dP}{dL} = \frac{2.88\,(1-\varepsilon)^{1.1}\,\mu^{0.1}\,\rho^{0.9}\,\bar{u}_s^{1.9}}{g_c\,\phi^{1.1}\,\varepsilon^3\,D_p^{1.1}} = k\bar{u}_s^{1.9} \qquad (2)$$

At intermediate flow rates, both viscous and kinetic effects are of approximately equal importance.

In order to make measurements of a cold flow simulating the flow through the porous bed of the combustion pot a smaller system of circular shape with a 5 in. ID was used (Figure 1), permitting smaller quantities of sample and avoiding air leakage. Pressure taps were drilled 4 in. apart up to a height of 20 in. High pressure air is fed through the bed of coke particles supported on a grate, with the air flow rate measured on a calibrated flow meter. The pressure drops through both systems are identical for the same bed height. Using these flow rates the pressure drops in fuel beds of different particle sizes have been measured.

Figure 2 shows the variation of pressure drop per unit length with velocity for several particle sizes. The non-linearity of the curve suggests that the flow in the system is not laminar. (For laminar flow, the pressure loss is proportional to the product of viscosity and the velocity through the bed, but for turbulent flow, from Equation 2 we expect to find $\Delta P/L$ proportional to $\bar{U}_S^{1.9}$.) Figure 3 illustrates the variation of $\Delta P/L$ with $\bar{U}_S^{1.9}$ indicating that the flow is turbulent. A log-log plot of $\Delta P/L$ against $\bar{U}_S$ yields an index of 1.86.

Whereas the flow in the bed had been assumed previously to be laminar since the Reynold's numbers were small (150-1000), the cold model experiments indicate that the flow is turbulent. That this difference has much effect on the reactions in the gasification zone is doubtful since the reactions depend predominantly on temperature, not flow characteristics. In the combustion zone the turbulence is much less significant than the laminar boundary layers around the particles. The study of the influence of the particle size on pressure drop will be continued. The use of the pressure drop as an index of the surface area will be investigated.

EFFECT OF HEATING RATE AND SOAK TEMPERATURE ON VOLATILE MATTER RELEASE

The computer modeling program for coal particle pyrolysis has been completed and a special report is in preparation. The reactor system to be used for the 1000°C/sec pyrolysis study has been completed and interfaced with a computer acquisition system. The overall system is now being tested.

The thermal model is being used to examine systematically the sensitivity of internal temperature profiles of coal particles to the following parameters:

1. heat transfer mechanism at particle surface;
2. thermal conductivity of particle;
3. particle size;
4. chemical reaction parameters;
   a. Arrhenius kinetic parameters;
   b. heat of reaction;
   c. initial concentration of pyrolytic material;
5. external driving temperature.

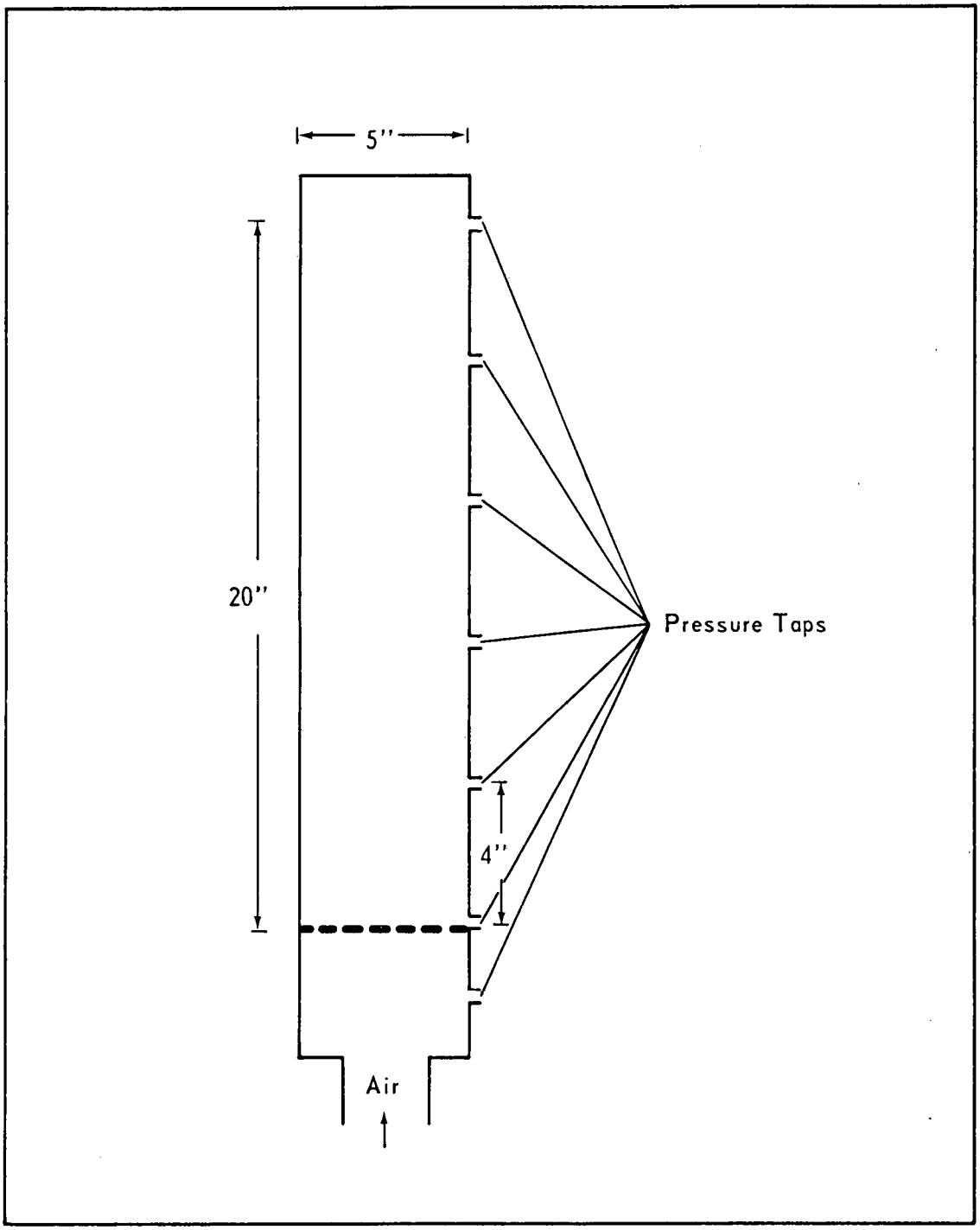

Figure 1 EXPERIMENTAL SYSTEM

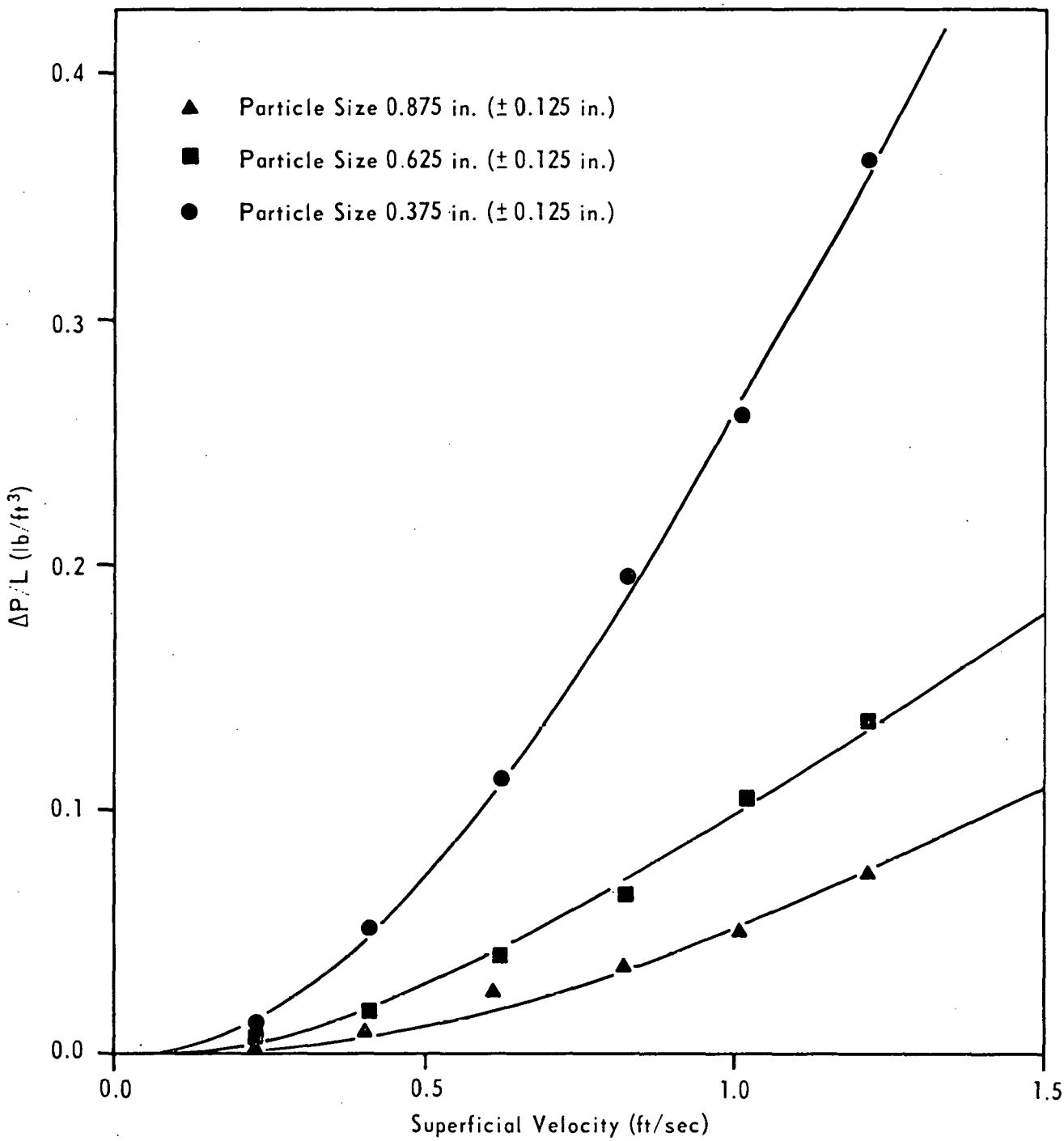

Figure 2 VARIATION OF ΔP/L WITH SUPERFICIAL VELOCITY IN AN EMPTY CONTAINER FOR THREE PARTICLE SIZES

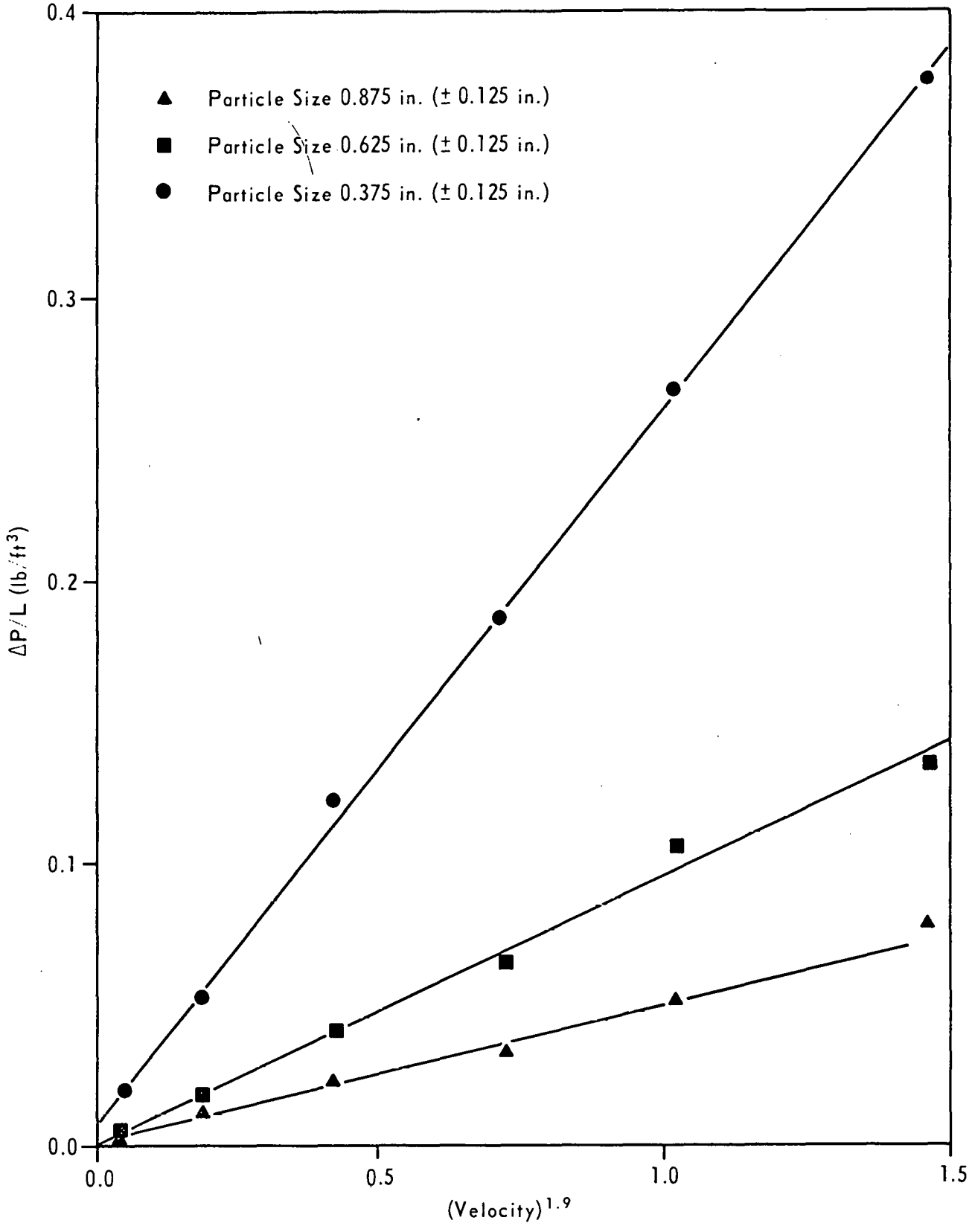

Figure 3 VARIATION OF ΔP/L WITH (VELOCITY)$^{1.9}$ FOR THREE PARTICLE SIZES

The computer model was used to develop a reactor system. The reactor was interfaced with the TOF mass spectrometer and preliminary pyrolysis runs indicate sufficient sensitivity. The mass spectrometer was interfaced with a mini- and a micro-computer system to facilitate rapid data acquisition. This system is being tested and presently can scan 120 mass peaks/sec.

CHARACTERISTICS OF CHARS PRODUCED BY PYROLYSIS FOLLOWING RAPID HEATING OF PULVERIZED COAL

Introduction

The characteristics of coal chars produced in atmospheres other than nitrogen were studied, using the same laminar flow furnace which has been described in previous progress reports. This phase has been started using air as the combustion medium and a North Dakota lignite (PSOC-246) as the starting parent coal. The work accomplished thus far involves: (i) grinding and studying of the particle size distributions of the particular size grades from PSOC-246, (ii) calibration of rotameters using air; and (iii) calculation of the theoretical air required for the complete combustion of PSOC-246 coal.

Experimental

Particle size distributions for PSOC-246 originally size graded to 270 x 400 mesh were studied using the method of dry sieve analysis. In this method, sieves of desired apertures are appropriately staged and a receiving pan is placed on the top sieve, which is then covered with a sieve cover. The contents are transferred to a Ro-Tap Sieve Shaker for screening. The weight retained on each sieve is accurately weighed (to four decimal places) and the cumulative weight percent greater than each screen aperture (equivalent to particle diameter) is obtained.

If the weight retained on the sieve of aperture x is denoted by R, then the particle size distributions of the particular size grade can be determined using the Rosin-Rammler relation[4]

$$R = 100 \exp [-(x/k)^n] \qquad (3)$$

where x and R are as defined before; k is a measure of the fineness of the material and when equal to x, $R = 100/e = 36.79$, and n is a measure of a size dispersion, a low value indicating a wide dispersion.

Equation (3) can be rearranged to

$$\ln[\ln(100/R)] = n \ln(x) + \text{constant} \qquad (4)$$

For a size distribution obeying the Rosin-Rammler relation, a plot of $\ln[\ln(100/R)]$ against $\ln(x)$ should give a straight line of slope n (as seen in Figure 4).

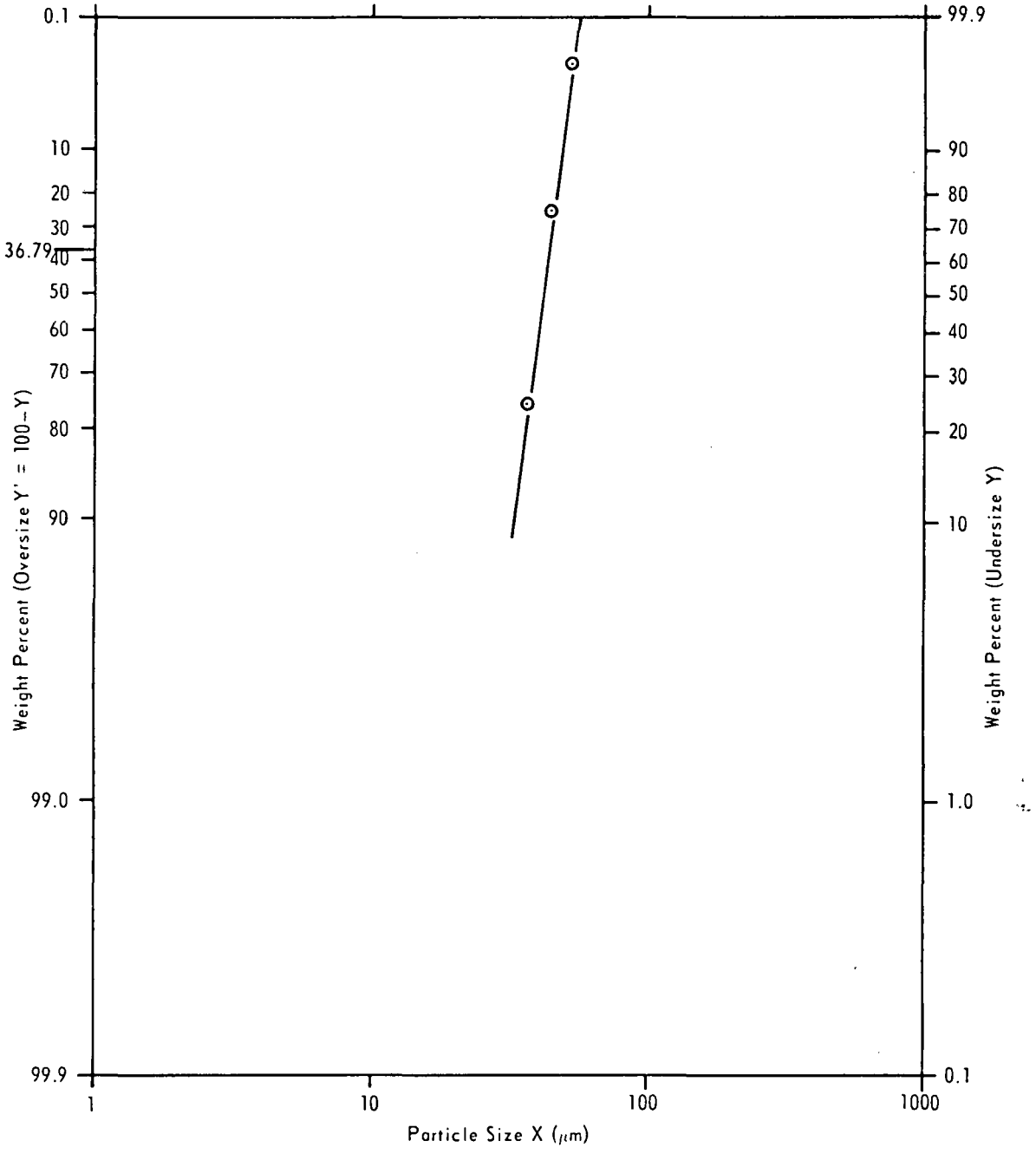

Figure 4 ROSIN-RAMMLER PLOT FOR PSOC-246 COAL ORIGINALLY SIZE GRADED TO 270 x 400 MESH

The weight mean size ($\bar{x}$) of particles is defined by[4]

$$\bar{x} = \int_0^\infty x \, dR \tag{5}$$

which gives, upon substituting R from Equation (3)

$$\bar{x} = [k][\phi(n)] \tag{6}$$

where $\phi(n)$ is the gamma function $\Gamma(1 + 1/n)$.

Five dry sieve analysis runs were made using the 270 x 400 mesh size grade of PSOC-246. The Rosin-Rammler parameters obtained as specified above are given below:

Run #	n	k	$\phi(n) = \Gamma(1 + 1/n)$	$\bar{x} = [k][\phi(n)]$
1	9.0	43	0.951	40.9
2	7.2	43	0.936	40.2
3	7.5	43	0.943	40.5
4	7.8	43	0.943	40.5
5	7.1	44	0.936	41.2

The accuracy with which the weight mean particle size ($\bar{x}$) could be determined was obtained from a statistical analysis based on the five observations shown above. Let N be the number of observations made. The mean value ($\bar{x}$) is by definition

$$\bar{x} = \Sigma X_i / N \tag{7}$$

and the standard deviation (S) is

$$S = \sqrt{(x_i - \bar{x})^2/(N - 1)} \tag{8}$$

The confidence interval ($\bar{x}_c$) is given by[5]

$$\bar{x}_c = \bar{x} \pm St/\sqrt{N} \tag{9}$$

where S anc $\bar{x}$ are as defined before, and t is the confidence factor; t varies with the number of observations and the degree of confidence desired. For example, for a 95 percent confidence interval based on five observations, t is equal to 2.8.

Based on a 95 percent confidence interval the value of the mean weight particle size could be determined to the accuracy of $\bar{x} = 40.7 \pm 0.5$ μm; that is, to about ± 1 percent.

Primary and secondary flow streams of air into the reaction zone of the laminar flow furnace are to be metered by Matheson #R-6-15-B and Air Products #09-1051 rotameters, respectively. These rotameters were calibrated with a wet test meter using air. The results are given in Figure 5. These curves are useful in deciding where to set the float of the rotameter when a particular volumetric flow of air is desired.

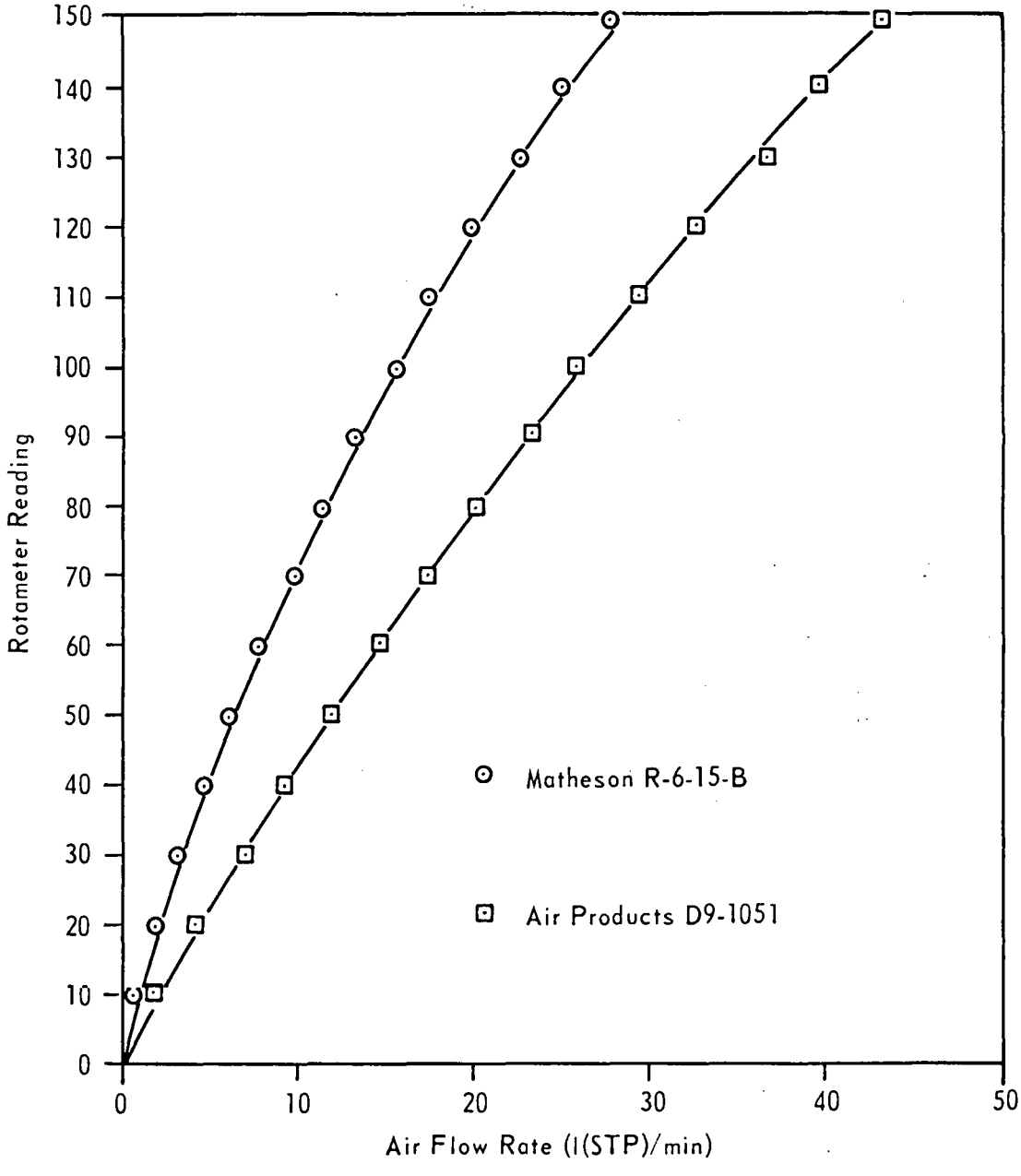

Figure 5 CALIBRATION OF ROTAMETERS USING AIR

Calculation of the quality of air theoretically required for the complete combustion of PSOC-246 follows. The chemical composition of the coal must be known. The composition of PSOC-246 is:

Constituent	Weight Percent (dry basis)
C	64.1
H_2	4.4
N_2	1.4
S	0.6
O	19.8
Ash	9.7

The chemistry of combustion involves the combination of carbon, hydrogen, and sulfur with oxygen as expressed by the following equations[6]:

$$C + O_2 = CO_2 \quad (10)$$

$$2H_2 + O_2 = H_2O \quad (11)$$

$$S + O_2 = SO_2 \quad (12)$$

From these equations (10-12), it is seen that 1 g of carbon, hydrogen, or sulfur requires for the conversion, during combustion, of carbon to carbon dioxide, hydrogen to water, or sulfur to sulfur dioxide, 2.67, 8, or 1 g of oxygen, respectively.

The amount of oxygen required by each chemical constituent per gram of fuel is calculated as follows:

Constituent	Weight of Constituent per Gram of Fuel	Weight of Oxygen Required per Gram of Fuel
C	0.641	0.641 x 2.67 = 1.711
H	0.044	0.0464 x 8 = 0.352
N	0.014	--
S	0.006	0.006 x 1 = 0.006
O	0.198	- 0.198 (initially present)
Ash	0.097	

Total weight of oxygen required per gram of fuel = 2.064 - 0.198 = 1.871 g (on dry basis) or 1.496 g on as fired basis (moisture in PSOC-246 is 20%).

Air consists of 23.2 parts of oxygen and 76.8 parts of nitrogen by weight. Therefore, the total air required is equal to $1.496 \times \frac{100}{23.2} = 6.45$ g. The density of air at 0°C and 760 torr is 1.293 g/l; hence, its specific volume is 1/1.293 = 0.773 l/g. Hence, the volume of air required per gram of PSOC-246 = 6.45 g x 0.773 l/g $\cong$ 5 l.

If, for example, PSOC-246 coal is fed into the reaction zone at 1 g/min, then a volumetric flow of air is 5 l/min would be required for stoichiometric conditions to exist. This flow rate can be obtained from Figure 5. However, complete combustion also depends on other factors, for example, particle size distributions, temperature/time history of the particles in the reaction zone, and diffusion limitations. Actually, complete combustion in this study is undesirable since the study is aimed at the elucidation of the characteristics of chars produced. Hence, the conditions of coal feed and air flow rates will be chosen such that this study can be conducted as a function of residence time, mean weight particle size, temperature, and fuel to oxidizer equivalent ratio.

METHANOL AND WATER DENSITIES OF COAL CHARS

Introduction

Water densities of a series of thirteen samples prepared from a lignite char were determined at 25°C. Water densities are very close to methanol and helium densities.

Experimental

Presented in this report are the results of water densities on the same set of char samples which were used previously for determining methanol densities. Water densities were determined at 25°C using pycnometers. For each sample, the densities (in duplicate) were determined after different intervals of contact time. The results are given in Table 4. The water densities show a drift with time, but for each sample constant values are obtained within 96 hr contact time. Furthermore, reproducibility of the data for duplicate runs for a given sample is good.

The 'equilibrium' water, methanol, and helium densities of various samples are given in Table 5. The water and methanol densities represent the average of the two determinations for each sample. It is seen that the water, methanol, and helium densities for a given sample are in excellent agreement. In no case do the methanol or water densities for a given sample differ from the helium density by more than 5 percent.

In order to further check the reproducibility of the water and methanol densities, nine determinations were made for methanol and water densities for a 1000°C lignite char (PSOC-138). Results are given in Table 6. For methanol, the mean density of the nine determinations is 1.667 g/cm^3. Standard deviation if 0.02187 g/cm^3, and for the nine determinations, a 95 percent confidence interval on the mean is 1.667 $\pm$ 0.015 g/cm^3. The corresponding values for the water density are 1.663 g/cm^3, 0.023 g/cm^3, and 1.663 $\pm$ 0.015 g/cm^3, respectively.

The results presented in this report strongly suggest that it is possible to determine the 'true' densities of chars using methanol and water. Densities of about twenty coals of different rank will be determined in water. These densities will be compared with helium densities.

Table 4. Helium and Water Densities of Chars

Sample		Water Densities g/cm³ (mmcb) After															
		2 hr		24 hr		48 hr		72 hr		96 hr		120 hr		144 hr		168 hr	
		1	2	1	2	1	2	1	2	1	2	1	2	1	2	1	2
	Carbon Deposited % (daf)	Carbon Deposition Series															
855°C Char	0	1.80	1.82	1.82	1.88	1.92	1.92	1.97	1.95	2.02	2.03	2.03	2.04	-	-	-	-
	1.0	1.84	1.85	1.87	1.89	1.92	1.94	1.95	1.99	1.97	2.00	-	-	1.98	2.00	-	-
	1.7	1.89	1.90	1.92	1.93	1.97	1.97	2.02	2.01	2.03	2.03	-	-	-	-	-	-
	2.6	1.80	1.87	1.81	1.88	1.90	1.91	-	-	-	-	1.92	1.92	-	-	-	-
1000°C Char	0	1.78	1.86	1.85	1.91	1.93	1.97	1.98	2.02	2.05	2.06	2.07	2.10	-	-	2.08	2.09
	3.6	1.89	1.77	1.91	1.85	1.91	1.98	1.94	1.93	1.98	1.97	2.00	2.00	-	-	2.01	2.02
	Burn-off % (daf)	Burn-off Series															
855°C Char	0	1.80	1.82	1.82	1.88	1.92	1.92	1.97	1.95	2.02	2.03	2.03	2.04	-	-	-	-
	1.1	1.87	1.88	1.95	1.94	1.99	1.95	2.03	2.04	2.06	2.06	2.05	2.05	-	-	-	-
	2.3	1.84	1.90	1.96	2.01	2.00	2.06	2.05	2.09	2.05	2.07	2.06	2.07	-	-	-	-
	10.2	1.95	1.90	1.98	1.92	2.05	2.01	2.12	2.10	-	-	2.13	2.11	-	-	-	-
	33.6	1.99	1.95	2.00	1.98	2.10	2.08	-	-	-	-	2.11	2.09	-	-	-	-
855°C Char-2.6% Carbon Deposited	0	1.82	1.79	1.88	1.84	1.90	1.87	1.93	1.92	1.93	1.95	1.93	1.94	1.92	1.94	-	-
	1.7	1.81	1.74	1.84	1.85	1.90	1.92	2.00	2.03	2.02	2.04	-	-	-	-	-	-
	3.7	1.80	1.84	1.88	1.91	1.98	20.4	2.04	2.04	2.04	2.06	-	-	2.04	2.04	-	-
	29.1	1.86	1.87	1.91	2.00	2.01	2.02	2.02	2.06	2.07	2.06	-	-	2.06	2.06	-	-

Table 5. Helium, Methanol and Water Densities of Chars

Sample		Density, g/cm³		
		Helium	Methanol	Water
	Carbon Deposited % (daf)	Carbon Deposition Series		
855°C Char	0	2.11	2.10	2.04
	1.0	1.90	2.09	1.99
	1.7	2.01	2.08	2.03
	2.6	1.88	1.90	1.92
1000°C Char	0	2.12	2.12	2.09
	3.6	2.04	2.05	2.02
	Burn-off % (daf)	Burn-off Series		
855°C Char	0	2.11	2.10	2.04
	1.1	2.07	2.11	2.05
	2.3	2.07	2.11	2.07
	10.2	2.16	2.14	2.12
	33.6	2.17	2.17	2.10
855°C Char 2.6% Carbon Deposited	0	1.88	1.88	1.94
	1.7	2.04	2.04	2.03
	3.7	2.00	2.06	2.05
	29.1	2.06	2.03	2.06

Table 6. Reproducibility of Methanol and Water Densities

Run No.	Methanol density (g/cm^3)	Water Density (g/cm^3)
1	1.686	1.675
2	1.687	1.680
3	1.645	1.679
4	1.667	1.643
5	1.681	1.638
6	1.673	1.681
7	1.635	1.676
8	1.638	1.667
9	1.689	1.630

EFFECT OF CARBON DEPOSITION ON THE POROSITY AND REACTIVITY OF CHARS

Introduction

The maximum amount of carbon deposition from the cracking of methane on the surface of a lignite char is much less than the amount of open pore volume which is potentially available to accomodate carbon. Carbon deposition reduces surface area and pore volume of the lignite char as well as accessibility of methane into the internal pore structure. This report describes the effect of carbon deposition within the pore volume of a lignite char on (1) changes in helium and mercury densities and pore volumes, and (2) ease of accessibility of methane into the internal pore structure.

Experimental

As discussed in the last progress report, a TGA unit was used for studying the kinetics of carbon deposition on the char. However, for measurement of surface area, helium and mercury densities as well as diffusion parameters, relatively larger quantities of samples are needed. Since carbon deposition in such quantities cannot be carried out in a conventional TGA unit, an alternate experimental approach was used for this purpose. About 4 g of the lignite char were taken in a graphite boat which was placed in a tube furnace. The system was purged with prepurified nitrogen for 1 hr. Heating was then started at a rate of 10°C/min. The sample temperature was raised to the desired carbon deposition temperature. Soak time at this temperature was 1 hr. Following this, nitrogen was replaced by the methane-nitrogen mixture. The extent of carbon deposition was estimated from the weight increase of the sample after the run.

Surface areas of various samples were determined from nitrogen adsorption at 77°K using the BET equation and from carbon dioxide adsorption at 298°K using the Polyanyi-Dubinin equation.[7] Adsorption isotherms were determined in a conventional volumetric apparatus.

In the present study, considerable time elapsed between the preparation of various char samples and their surface area measurements. In a few preliminary runs, it was found that heat treatment/outgassing conditions prior to surface area measurements profoundly affected the surface area values, particularly the nitrogen surface areas. The higher the heat treatment/outgassing temperature, the larger was the surface area. The following reasoning seems to be plausible for explaining these results. The chars are turbostratic carbons. Therefore, they are expected to have a reasonable concentration of carbon sites located at the edges of layer planes. These sites can potentially chemisorb oxygen on exposure to air even at ambient temperature.[8,9] Therefore, when a freshly prepared char is exposed to air, it can chemisorb oxygen. Since most of the area of chars is located in micropores, the chemisorption of oxygen is expected to decrease the micropore size to an extent that some of the micropores initially present in the char will become inaccessible to adsorbate molecules. Since the minimum dimension of a nitrogen molecule (3.64Å) is larger than that of a carbon dioxide molecule (3.3Å), the chemisorption of oxygen is expected to adversely affect the nitrogen area to a greater extent than the carbon dioxide area. Heat treatment (or outgassing) of a char at progressively increasing temperatures will desorb increasing amounts of chemisorbed oxygen. Therefore, porosity of a char will increase with increasing heat treatment temperature provided the temperature does not exceed that seen by the char during its preparation. With increase in porosity, accessibility of pores to the adsorbate molecules will increase. This in turn will result in an increase in surface area. Therefore, in order to avoid any ambiguity in the surface area values, the following procedure was used. Before making an adsorption run, the sample was heated in a tube furnace for 2 hr in a prepurified nitrogen flow at a temperature 50°C below that seen by the sample during its preparation. Thereafter, the sample was cooled in nitrogen to room temperature. A known amount of the sample was immediately transferred to a sample holder which was then attached to the adsorption equipment. Prior to measuring the surface area, the sample was again outgassed at 500°C for 8 hr. For each adsorption point on the nitrogen and carbon dioxide isotherms, an arbitrary adsorption time of 30 min was allowed.

True and apparent densities of various samples were determined by helium and mercury displacements, respectively, in the manner described previously.[7] These densities were used to calculate the open pore volumes and percentage porosities.[7]

The desorption technique described by Walker and co-workers[10,11] was used to measure the diffusion parameter for methane. The apparatus as well as the experimental and computational procedures used to calculate the diffusional parameter $D^{1/2}/r_o$ (where D is the diffusional coefficient and r_o is the diffusion path length) have been described in detail by Nandi and Walker.[11]

Prior to making a diffusion run, the char sample was subjected to the same heat treatment cycle as was used for surface area measurements. The sample was then equilibrated with about 400 psi methane for 24 hr. This time was ascertained in a few exploratory runs to be sufficient for the attainment of equilibrium. The volume of methane desorbed after different time intervals

was determined in the manner described previously.[11] The following equation, applicable far from equilibrium, was used to calculate the diffusion parameter:[10,11]

$$\frac{V_t - V_o}{V_\infty - V_o} = \frac{6}{\sqrt{\pi}} \left(Dt/r_o^2\right)^{1/2} \qquad (13)$$

where V_∞, V_t, and V_o are the volumes of methane desorbed after time $t = \infty$, $t = t$, and $t = 0$, respectively. The volume of methane desorbed after 24 hr was taken as V_∞. Plots of $(V_t - V_o)/(V_\infty - V_o)$ against $t^{1/2}$ give straight lines; the slopes were used to calculate diffusion parameters.

The nitrogen and carbon dioxide surface areas of various samples are given in Table 7. Considering the results for the char samples, it is seen that the areas decrease progressively with increasing amounts of carbon deposition. The effect of gasification on surface area is different for the raw and carbon deposited chars. In the former case, nitrogen area increases whereas carbon dioxide area decreases with increasing carbon burn-off. However, gasification of the carbon deposition samples results in an increase in both nitrogen and carbon dioxide areas. It is noted that even after 2.6 percent carbon deposited char is activated to 29.1 percent burn-off, the nitrogen and carbon dioxide areas are not 'restored' to the areas of the raw char.

Except in the case of the 855°C char activated to 33.6 percent burn-off, which has about the same nitrogen and carbon dioxide areas, the nitrogen areas for the remainder of the carbon deposited and activated char samples are less than the corresponding carbon dioxide areas. The lower nitrogen areas are presumable due to activated diffusion into the microporous structure[12] such that more of the ultra-fine micropores are inaccessible to nitrogen than carbon dioxide.

The nitrogen and carbon dioxide areas of the activated carbon also decrease upon carbon deposition (Table 7). The decrease in area upon carbon deposition is less pronounced for the activated carbon than for the char samples. For instance, 2.6 percent carbon deposited on the 855°C char decreased the carbon dioxide area from 960 to 249 m^2/g, whereas 13.3 percent carbon deposited on the activated carbon decreases the carbon dioxide area from 838 to only 679 m^2/g. For the activated carbon, nitrogen areas are higher than the carbon dioxide areas at each level of carbon deposited. This phenomenon has previously been reported for various microporous carbons.[13] The higher nitrogen areas have been attributed to reversible filling of micropores. It has been argued that such nitrogen areas are often meaningless.[13]

Helium and mercury densities, total open pore volumes and open porosities of various samples are listed in Table 7. Porosity decreases following carbon deposition and increases upon activation. Assuming that the density of the deposited carbon is essentially the same as that of the carbon in the raw lignite char, the maximum amount of carbon deposited is substantially less than that which could be accomodated within the open pore volume of the char. For example, the 855°C raw char had an open porosity of 35.6 percent (Table 7), but maximum carbon deposited was only 2.6 percent.

Microporous carbon solids appear to be without exception aperture-cavity type materials.[14] Results on the effect of carbon deposition on open

Table 7. Area, Density, and Porosity Data for Various Samples

Sample		Surface Area m^2/g(daf) N_2	Surface Area m^2/g(daf) CO_2	Helium Density gcm^{-3}(daf)	Mercury Density gcm^{-3}(daf)	Open Pore Volume cm^3g^{-1}(daf)	Open Porosity (%)
	Carbon Deposited % (daf)	Carbon Deposition Series					
855°C Char	0	241	960	2.05	1.32	0.270	35.6
	1.7	76	771	1.94	1.37	0.214	29.3
	2.6	33	249	1.80	1.37	0.174	23.8
1000°C Char	0	130	681	2.06	1.36	0.250	34.0
	3.6	31	457	1.98	1.35	0.236	31.9
BPL Carbon	0	1296	838	2.1	0.85	0.700	59.5
	2.4	1030	745	-	-	-	-
	5.2	916	726	-	-	-	-
	13.3	807	679	-	-	-	-
	Burn-off % (daf)	Burn-off Series					
855°C Char	0	241	960	2.05	1.32	0.270	35.6
	1.1	336	799	2.01	1.28	0.284	36.3
	2.3	385	800	2.01	1.26	0.296	37.3
	10.2	484	747	2.10	1.26	0.324	40.5
	33.6	695	699	2.09	1.06	0.465	49.3
855°C Char-2.6% Carbon Deposited	0	33	249	1.80	1.37	0.174	23.8
	1.7	43	339	1.98	1.31	0.258	33.8
	3.7	124	361	1.97	1.28	0.270	34.5
	29.1	160	369	1.98	1.22	0.314	38.4

porosity in the lignite char are consistent with this conclusion. As seen in Table 7, deposition of 2.6 percent by weight, carbon leads to a reduction in open porosity from 35.6 to 23.8 percent. It is obvious that some apertures are being reduced in size by carbon deposition to the extent that helium no longer can pass through at room temperature. Thus, the accessibility of helium to the larger cavities existing behind the apertures has been removed, leading to a reduction in porosity considerably in excess of the total volume of carbon which has been deposited. Extensive subsequent gasification of the carbon deposition raw char does not open up porosity to the extent that is found for gasification of the raw char. Again, see Table 7, gasification to about 30 percent burn-off produces an open porosity in the 855°C raw char of 49.3 percent but only 38.4 percent within the carbon deposited-raw lignite char. This is consistent with the reactivity of the deposited carbon being significantly less than that of the lignite char carbon.

It was observed in a few preliminary runs that in the case of the 855°C char activated to more than 2 percent burn-off and for the 2.5 percent carbon deposited char activated to 29.1 percent burn-off, diffusion of methane was so rapid that diffusion parameters could not be estimated. Therefore, diffusion parameters could only be estimated for selected samples. Diffusion of methane from some samples was also measured as a function of temperature in order to obtain information on whether diffusion was activated.

Typical methane diffusion plots are shown in Figure 6. Diffusion parameters are listed in Table 8. To calculate D values, the average particle radius (that is, 0.0142 cm) was arbitrarily taken for r_o. These data indicate that deposition of carbon on the char reduces the diffusion parameter, whereas gasification of the raw as well as the carbon deposition chars increases the diffusion parameter. Furthermore, diffusion is non-activated on the 855°C char but is activated on the char following either carbon deposition to 2.6 percent (that is, 4.7 ± 1.1 kcal/mole) or carbon deposition to 2.6 percent and burn-off to 3.7 percent (that is, 2.3 ± 0.9 kcal/mole).

The diffusion results support the porosity changes resulting from carbon deposition and carbon burn-off. The diffusion coefficient decreases and activation energy for diffusion increases following carbon deposition due to reduction in aperture sizes. The enlargement of apertures following carbon burn-off results in an increase in the diffusion coefficient and a decrease in the activation energy. That the deposited carbon is less reactive during gasification than the base lignite char carbon is indicated by a lower diffusion coefficient for the 2.6 percent carbon deposited-3.7 percent burn-off char, representing a net burn-off of 1.1 percent, compared to that for the 1.1 percent burn-off raw char. Any changes in diffusion coefficient resulting from carbon deposition are expected to affect the utilization factor during subsequent gasification of the char.[15] The effect of carbon deposition within the pore volume of the lignite char on subsequent gasification in air will be studied next.

Table 8. Diffusion Results at Various Measurement Temperatures

Sample	-15°C		0°C		25°C		40°C	
	$D^{1/2}/r_o \times 10^3$ ($sec^{-1/2}$)	$D \times 10^9$ ($cm^2 sec^{-1}$)	$D^{1/2}/r_o \times 10^3$ ($sec^{-1/2}$)	$D \times 10^9$ ($cm^2 sec^{-1}$)	$D^{1/2}/r_o \times 10^3$ ($sec^{-1/2}$)	$D \times 10^9$ ($cm^2 sec^{-1}$)	$D^{1/2}/r_o \times 10^3$ ($sec^{-1/2}$)	$D \times 10^9$ ($cm^2 sec^{-1}$)
855°C Raw Char	6.21	7.80	6.48	8.49	6.40	8.28	-	-
1.7% Carbon Deposited	-	-	-	-	3.00	1.82	-	-
2.6% Carbon Deposited	-	-	2.05	0.85	2.53	1.55	3.51	2.49
1.1% burn-off	-	-	-	-	8.92	16.1	-	-
2.6% Carbon Deposited- 1.7% burn-off	-	-	-	-	2.77	6.97	-	-
2.6% Carbon Deposited 3.7% burn-off	5.72	6.62	6.17	7.70	7.81	12.3	-	-
1000°C Raw Char	-	-	-	-	4.95	4.94	-	-
3.6% Carbon Deposited	-	-	-	-	3.00	1.82	-	-

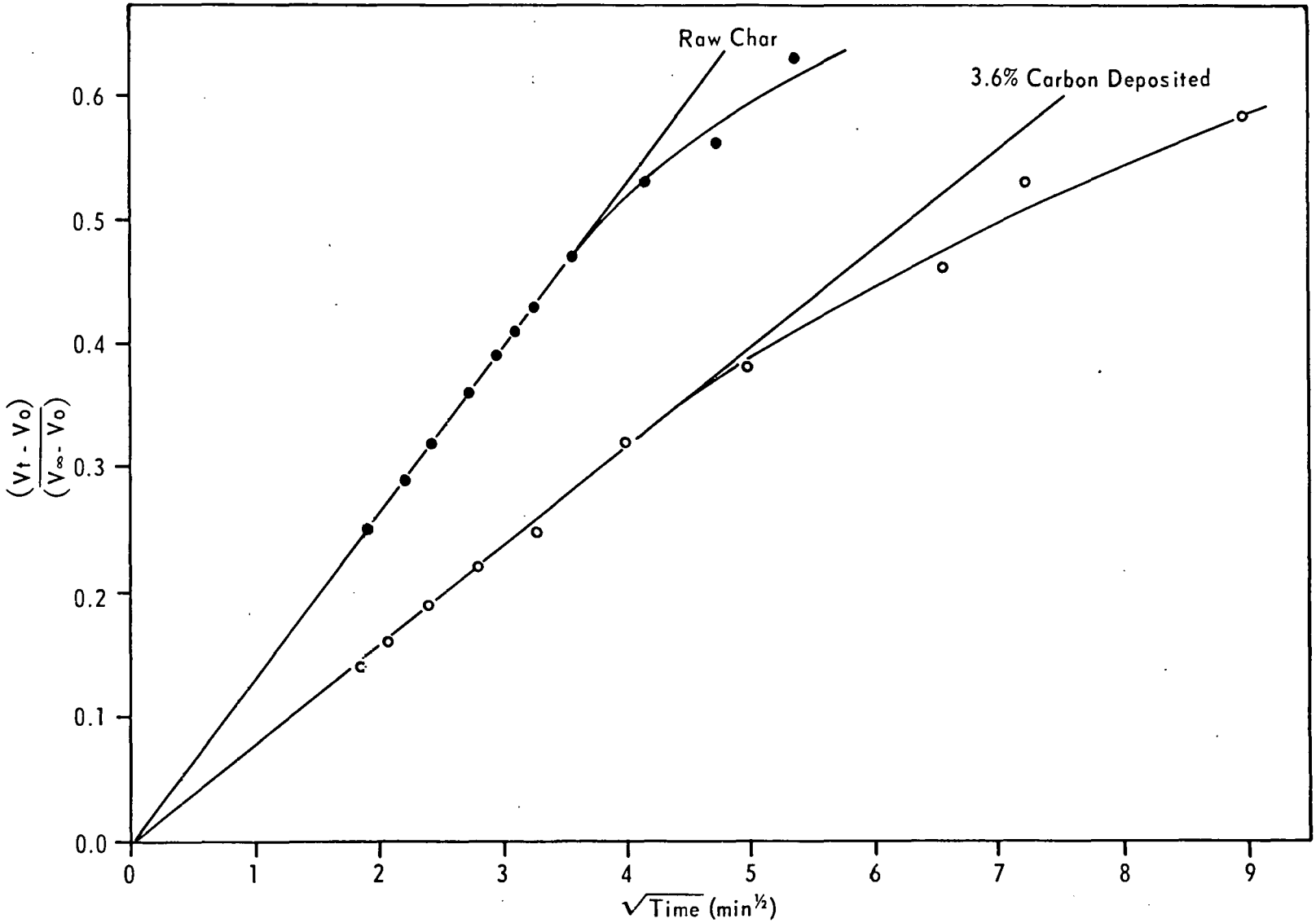

Figure 6 METHANE DESORPTION PLOTS FOR RAW AND CD 1000°C CHARS

CHEMISORPTION OF OXYGEN ON CARBONACEOUS SOLIDS

Introduction

The DSC and TGA techniques were used to calculate the heat of chemisorption of oxygen, ΔH, on two Saran carbons. The values of ΔH were 38 ± 2 and 70 ± 2 kcal/mole oxygen for the unactivated and the oxygen-activated carbon, respectively. Chemisorption was found to be associated with a physical adsorption process at lower reaction temperatures and a gasification reaction at higher temperatures.

Experimental

This report describes further studies on thermal effects involved during chemisorption of oxygen on Saran carbons. Both DSC and TGA techniques have been used. For the chemisorption process occurring at a particular moment, the quantity of heat, Q, released per g of carbon is determined by the former technique. Under the same experimental conditions, a TGA unit is used to measure W, the amount of oxygen uptake per g of carbon. The heat of chemisorption, ΔH, is computed by using the relation:

$$\Delta H = \frac{Q}{W} \times 32 \qquad (14)$$

where ΔH = kcal/mole oxygen chemisorbed
Q = cal/g carbon
W = g oxygen chemisorbed/g carbon

Experiments were conducted in the temperature range 75-227°C. In all cases, values of ΔH were computed at several time intervals between 2 and 28 min. The zero time is defined here as the time when the oxidant gas comes in contact with the carbon surface. After replacing nitrogen by oxygen, it takes about 2 min for the oxygen to displace nitrogen near the carbon surface. Two Saran carbon samples have been studied: (1) the unactivated sample (150 x 250 mesh size) associated with 18-22 ppm iron as an impurity, and (2) the unactivated sample activated to 63.8 percent carbon burnoff in an oxygen atmosphere. For the former sample, values of ΔH were obtained at 100, 125, 150, 177, 202, and 227°C. At 100°C, ΔH, over the time interval considered, was essentially constant and amounted to 38-40 kcal/mole. At higher temperature, however, ΔH increased with time (Figure 7). The spread of ΔH values increased with temperature from 38-50 kcal/mole at 150°C to 102-156 kcal/mole at 227°C. It is believed that for the unactivated sample for reaction above 100°C, chemisorption of oxygen is also accompanied by gasification. During the reaction, the sample weight increases because of chemisorption, but at the same time it decreases due to gasification. Since both reactions occur simultaneously, the observed weight change recorded by the TGA unit is in fact the difference between the weight gained due to chemisorption and that lost due to gasification.

In order to avoid the possibility of the occurrence of gasification during chemisorption, it was thought advisable to work at relatively lower temperatures, preferably below 100°C. However, below 100°C, the area of

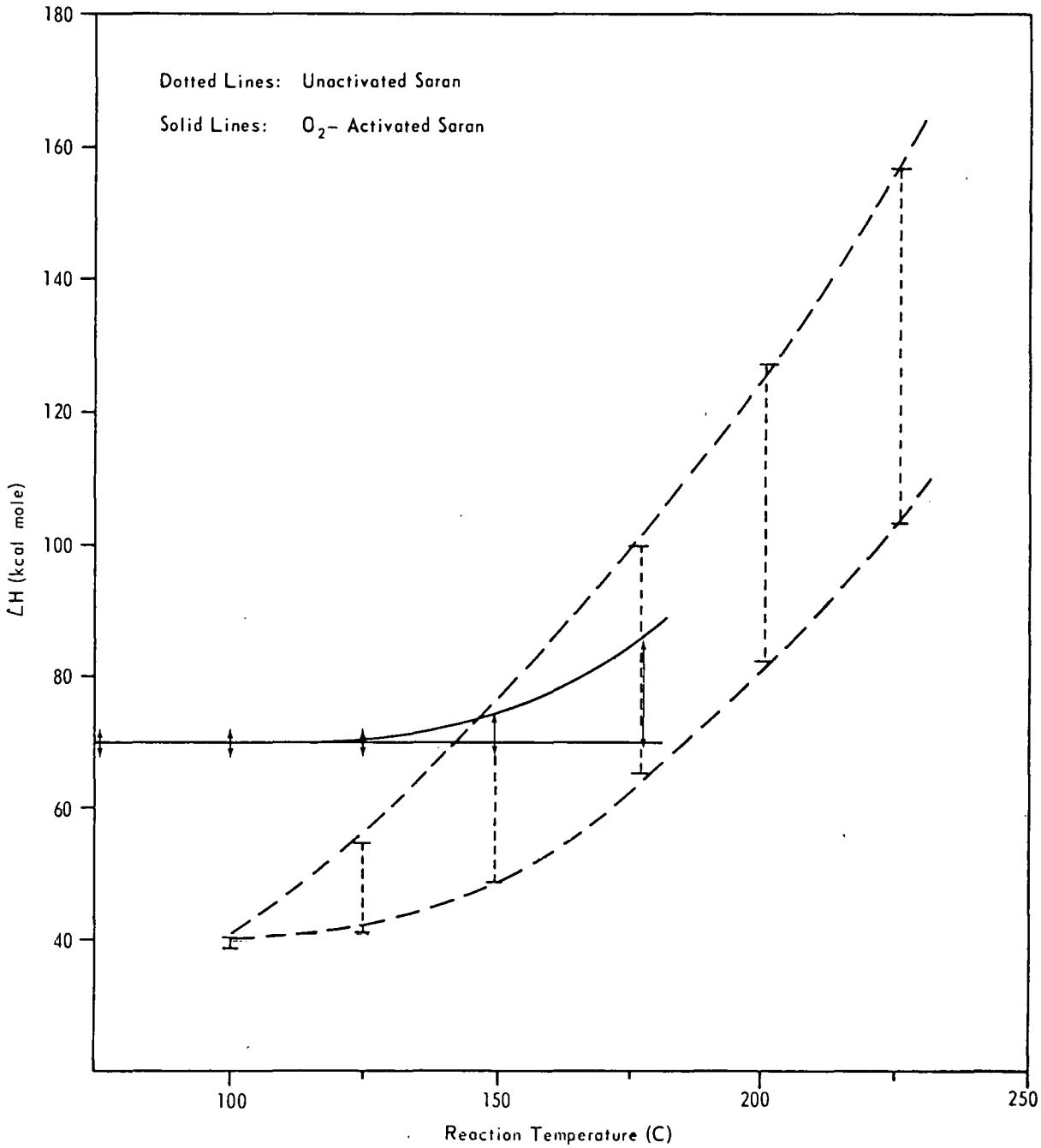

Figure 7 VARIATION OF ΔH WITH REACTION TEMPERATURE

the thermogram obtained during the DSC scan was small and thus no meaningful conclusions regarding ΔH could be drawn. Therefore, it was necessary to use a sample which had a higher rate of oxygen chemisorption. For this study, the oxygen-activated sample was used. Values of Q and W were determined at 75, 100, 125, 150, 177, and 202°C. In all cases, it was observed that the higher the reaction temperature, the higher was the value of Q. However, the W values at 177°C were higher than those at 202°C (Figure 8, plots V and VI). This indicates that at 202°C, the rate of gasification is relatively higher compared to that of chemisorption. The net result is, therefore, a lower value of W at 202°C than at 177°C. Besides, below 177°C, neither the DSC technique nor the TGA technique can indicate whether gasification is occurring or not. However, an increase in the ΔH values with reaction temperature is indicative of the occurrence of gasification.

Figure 9 shows the dependence of ΔH on reaction time and temperature. At 75°C, ΔH increases from 50 kcal/mole after 2 min to 64 kcal/mole after 15 min reaction time. Thereafter, ΔH remains essentially constant. At 100 and 125°C, the values of ΔH are scattered around an average value of 70 2 kcal/mole. These ΔH values are essentially independent of reaction time or temperature. At 150°C, during the first 10 min ΔH has a constant value of 70 kcal/mole which increases to 72, 74, and 77 kcal/mole after 15, 20, and 25 min reaction time, respectively. This suggests that at 150°C gasification starts about 15 min after introducing oxygen. The results also suggest that at 177°C, gasification starts after about 4 min.

At 75°C, the observed variation of ΔH with reaction time is indicative of the simultaneous occurrence of physical adsorption which is known to be more pronounced at lower temperatures. The extent of physical adsorption on the carbon was studied in the following manner. The carbon was first exposed to oxygen at 100°C for 48 hr. It was ascertained that a further increase in reaction time had no additional effect on weight change of the sample. The sample was then outgassed and finally flushed with nitrogen at 75°C. Thereafter, nitrogen was replaced by oxygen at the same reaction temperature. An increase in weight of the sample was ascribed to physical adsorption of oxygen (W_P). This increase in weight was monitored as a function of time. Table 9 lists the values of W_P as well as the total oxygen adsorbed, W_T, that is the sum of physisorbed and chemisorbed oxygen. The amount of chemisorbed oxygen, W_C, was calculated by the following relationship

$$W_C = W_T - W_P \tag{15}$$

The use of W_T and W_C values gives $\Delta H'$ and ΔH values respectively, which are listed in Table 9. It is noteworthy that the first four values of H give n average value of $\Delta H = 66.7$ kcal/mole, while the last four values are scattered around 72.2 kcal/mole. The difference between the two, that is, 5.5 kcal/mole, could be considered to represent the heat of physical adsorption, which cannot be determined directly by the DSC technique.

In order to further understand the gasification process, two different approaches were considered. In the first approach, following heat treatment at 600°C, the activated sample was exposed to oxygen at 202°C for 28 min in the TGA unit. Nitrogen was then passed over the sample. The sample weight

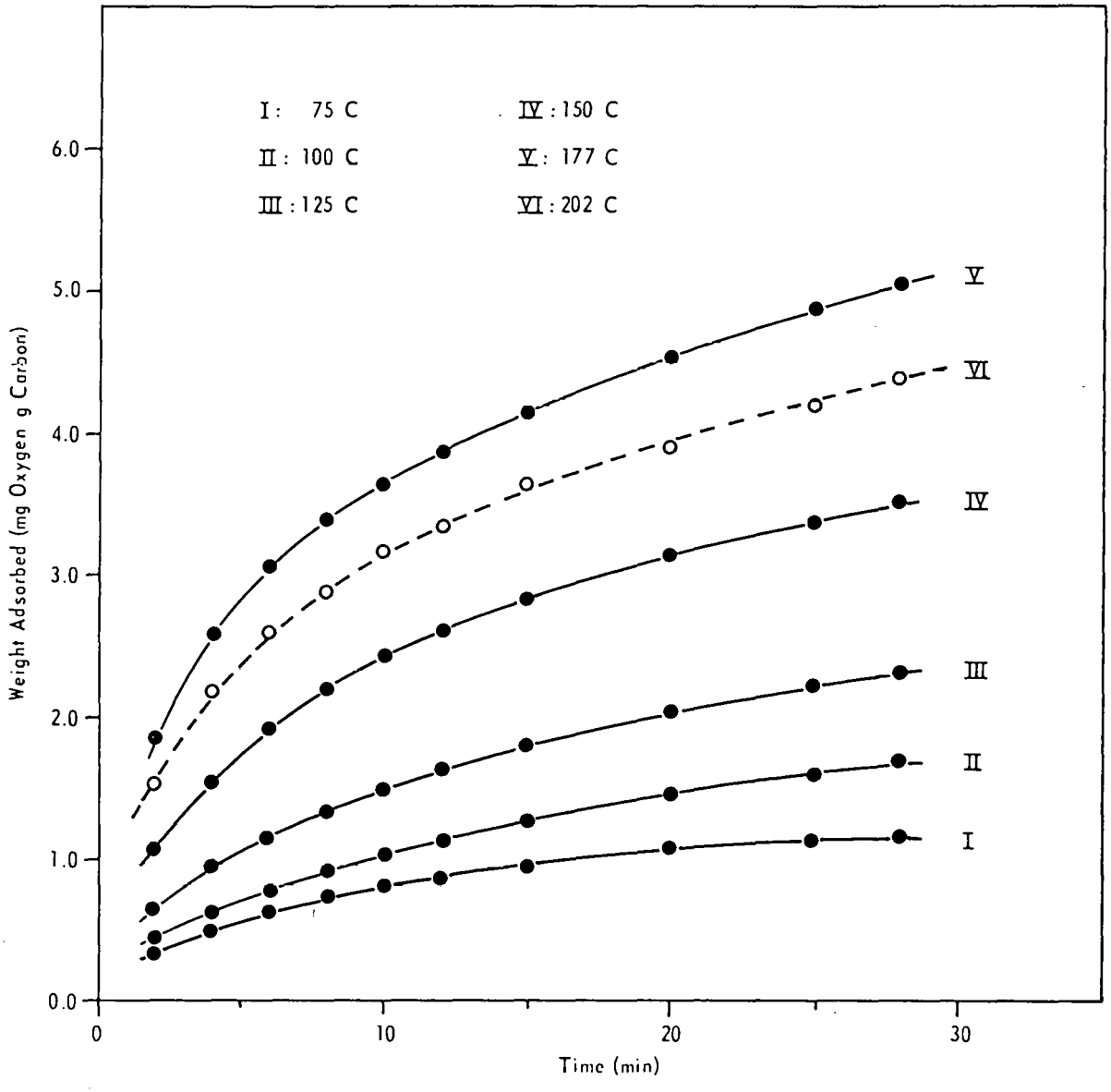

Figure 8 AMOUNT OF OXYGEN UPTAKE ON THE ACTIVATED SARAN CARBON

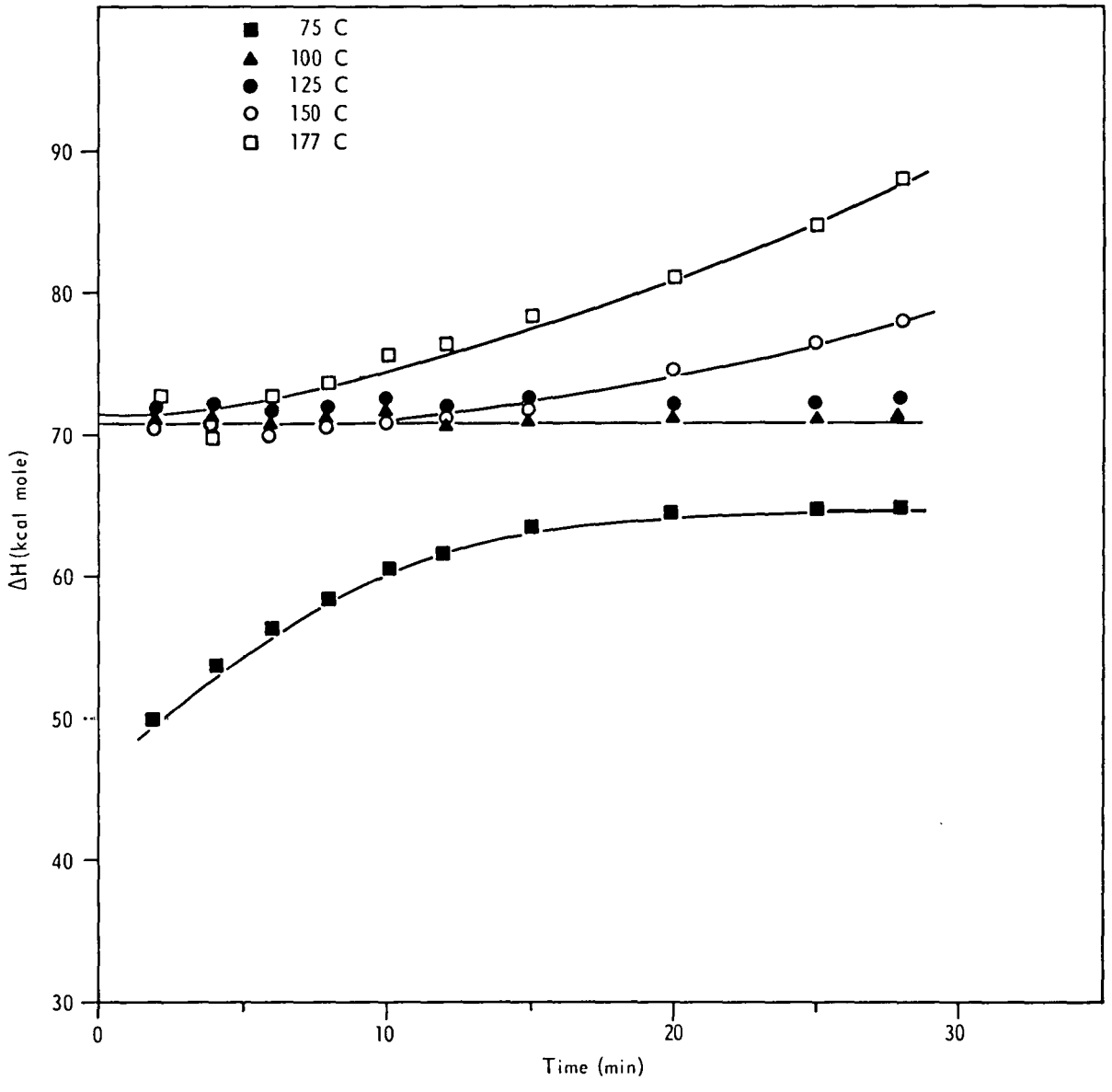

Figure 9 DEPENDENCE OF ΔH ON REACTION TEMPERATURE AND TIME FOR THE ACTIVATED SARAN CHAR SAMPLE

Table 9. Physisorption and Chemisorption of Oxygen on Activated Saran Carbon at 75°C

	t(min)	Q(cal/gC)	W_t (mg O_2/gC)	ΔH' (kcal/mole)	W_P (mg O_2/gC)	W_C* (mg O_2/gC)	ΔH (kcal/mole)
1	2	0.534	0.346	49.4	0.089	0.257	66.5
2	4	0.890	0.519	54.8	0.093	0.426	66.9
3	6	1.123	0.635	56.6	0.096	0.539	66.7
4	8	1.318	0.727	58.0	0.104	0.623	67.7
5	10	1.486	0.785	60.6	0.107	0.678	70.1
6	12	1.635	0.855	61.2	0.111	0.744	70.3
7	15	1.825	0.923	63.2	0.114	0.809	72.2
8	20	2.074	1.028	64.6	0.114	0.914	72.6
9	25	2.287	1.132	64.7	0.114	1.018	71.9
10	28	2.398	1.189	64.5	0.114	1.075	71.4

*$W_C = W_T - W_P$

remained unchanged for a period of 3 hr. This indicates that in the presence of oxygen gasification occurs simultaneously with chemisorption. It is well known that the first step in the overall gasification process is the dissociative chemisorption of the reactant gas. During oxygen chemisorption, two types of complexes are formed on the carbon surface, a stable complex, and a fleeting carbon-oxygen complex. The fact that heat treatment of the oxygen-treated sample in nitrogen did not involve any weight loss shows that the "stable" carbon-oxygen complex formed during chemisorption is thermally stable in an inert atmosphere at the temperature at which oxygen was initially chemisorbed.

In the second approach, a few mathematical calculations were made on the data obtained with the activated sample. At 75, 100, and 125°C, chemisorption is the only process involved because the value of ΔH (70 ± 2 kcal/mole) is independent of reaction time or temperature. Therefore, it is reasonable to assume that at 150 and 177°C, the same value of ΔH would be obtained if no gasification were taking place. In other words, the chemisorption process is governed by

$$(\Delta H)_{t,T} = 32\ (Q/W)_{t,T} = \text{const} = 70 \text{ kcal/mole} \qquad (16)$$

where t = 2-28 min
T = 75-177°C

When gasification occurs, the experimental value of weight gained, W_T, is less than what it would have been if the process involved only chemisorption.

Thus, if W_C is the calculated weight of oxygen required for ΔH = 70 kcal/mole, then the weight loss during gasification, W_g, is given by

$$W_g = W_C = W_T \qquad (17)$$

Values of W_C were calculated at t > 10 min at 150°C, and t > 4 min at 177°C, and are listed in Table 10. These calculations were performed in the following manner. For each data point, the experimental value of Q was substituted in Equation (16) to obtain the corresponding value of W_C. No correction was made to account for contributions to Q from the gasification process. It is clear from Table 10 that the values of W_g increase with reaction time or temperature, as expected.

The total area accessible to oxygen chemisorption will be determined by using the mass spectrometer and TGA techniques. The dependence of heat of chemisorption on surface coverage will be investigated also.

Table 10. Calculated Values of the Weight Gasified*

	150°C			177°C		
(minutes)	W_C	W_t	W_g	W_C	W_t	W_g
6	-	-	-	3.173	3.049	0.124
8	-	-	-	3.639	3.415	0.224
10	-	-	-	4.043	3.660	0.383
12	-	-	-	4.395	3.902	0.493
15	2.990	2.868	0.122	4.851	4.187	0.664
20	3.383	3.163	0.220	5.535	4.553	0.982
25	3.689	3.379	0.310	6.110	4.878	1.232
28	3.844	3.536	0.308	6.405	4.081	1.324

*mg gasified/g carbon

CATALYTIC ACTIVITY OF MINERALS FOR THE CRACKING OF METHANE

Introduction

The phenomenon of chemical vapor deposition resulting from the cracking of methane on various surfaces has been reported widely in the literature. It has recently been shown in this laboratory that mineral matter associated with the chars catalyzes the cracking of methane. It is, therefore, of interest to know which specific major mineral(s) present in chars (as a result of being in the coal precursors) catalyze the cracking of methane. We have investigated the possible catalytic activity of major minerals present

in coals, namely, kaolinite, illite, calcite, dolomite, quartz, gypsum, rutile, pyrite, and siderite, for the cracking of methane.

Experimental

The following minerals obtained from Ward's Natural Science Establishment, Inc., New York, were used in this study:

Mineral	Location	Chemical Formula
Kaolinite	Bath, S.C.	$Al_4SI_4O_{10}(OH)_6$
Illite	Fithian, Ill.	$K_4(Al,Fe)_V(Mg,Fe)_WSi_XAl_YO_{10}(OH)_2$
Calcite	Chihuahua, Mexico	$CaCO_3$
Dolomite	Elzevir, Ontario	$CaCO_3 \cdot MgCO_3$
Quartz	Minas Gerais, Brazil	SiO_2
Gypsum	Washington, Utah	$CaSO_4 \cdot 2H_2O$
Rutile	Gaston, N.C.	TiO_2
Pyrite	Rico, Colorado	FeS_2
Siderite	Nova Scotia, Canada	$FeCO_3$

The various minerals were ground and -325 mesh fractions used in the present study.

To study the rate of methane cracking on minerals, a Fisher TGA unit, series 300, was used. About 10 mg of a mineral contained in a platinum pan were heated in a nitrogen flow (500 cc/min) up to 900°C at a rate of 20°C/min. Soak time at 900°C was 30 min after which nitrogen was replaced by a mixture of methane and nitrogen at a total pressure of 1 atm and a methane partial pressure of 50 torr.

With the exception of quartz and rutile, the remainder of the minerals were found to undergo thermal decomposition upon heat treatment up to 910°C in a nitrogen atmosphere.

Of all the minerals studied, only two minerals, namely siderite and calcite were found to be catalysts for the cracking of methane; the catalytic activity was much more pronounced for siderite. Gypsum was found to 'react' with methane although no carbon deposition was observed on the surface.

During heat treatment in a nitrogen atmosphere, siderite loses carbon dioxide between 400 to 600°C, the weight loss corresponds to the conversion: $FeCO_3 \rightarrow FeO + CO_2$ (Figure 10). Between 600 to 900°C, no additional weight changes are observed. At 900°C, nitrogen is replaced by the methane-nitrogen mixture at the same flow rate. Upon introduction of the mixture, a sharp decrease in weight is observed which corresponds to the transition $FeO \rightarrow Fe$. Thereafter, a continuous increase in weight is observed (Figures 10-12). The maximum rate of weight increase is 0.11 mg hr^{-1} mg^{-1} starting weight of siderite. These results indicate that the catalytic activity of siderite for the cracking of methane is due to the formation of elemental iron. In order to confirm this, the following experiment was performed. After the thermal decomposition of siderite to FeO, nitrogen was replaced by a nitrogen-hydrogen mixture containing hydrogen at a partial pressure of 150 torr. The system was then heated up to 900°C in the nitrogen-hydrogen atmosphere.

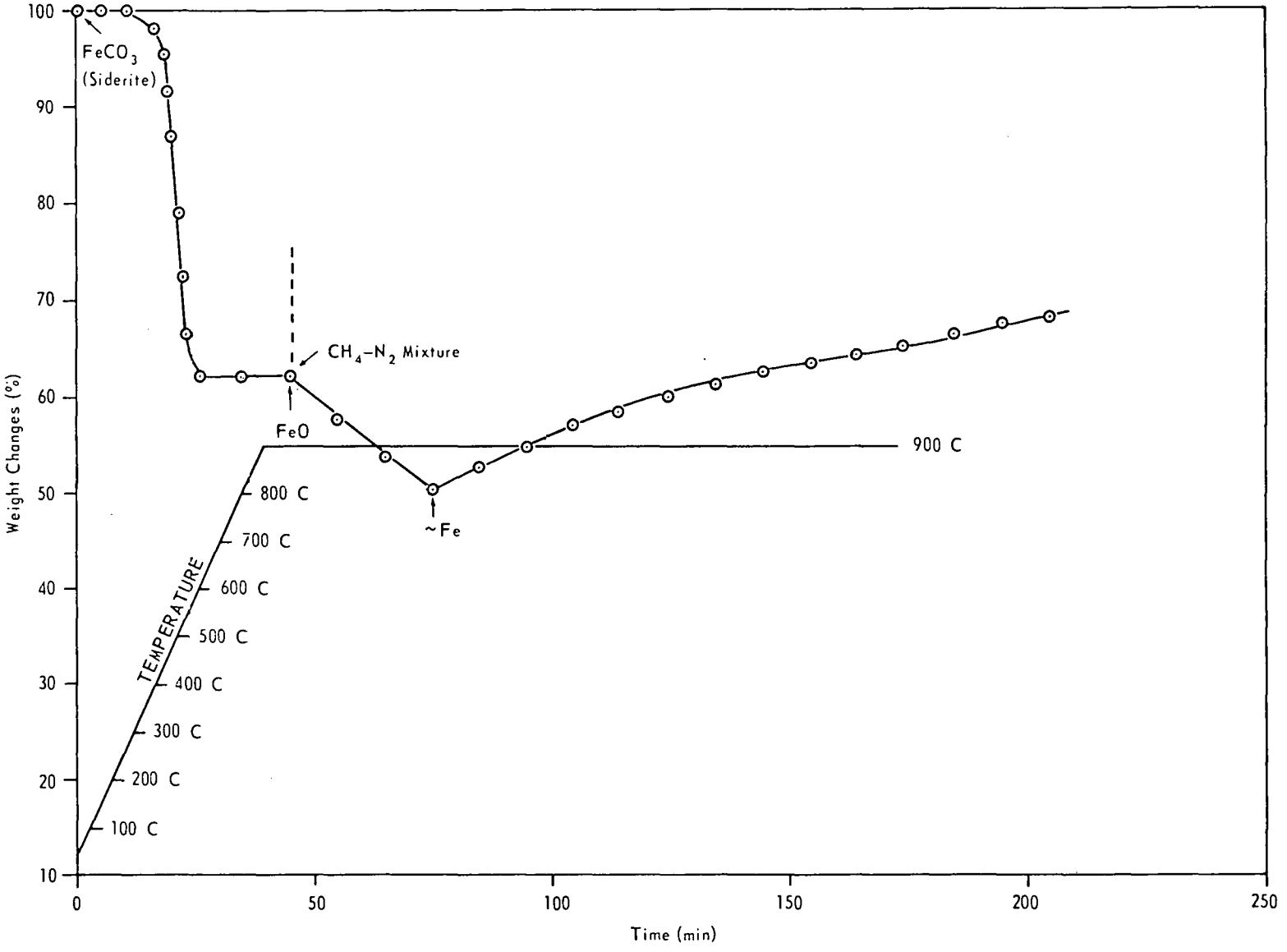

Figure 10 WEIGHT CHANGES OCCURRING DURING HEAT TREATMENT AND CRACKING OF METHANE ON SIDERITE

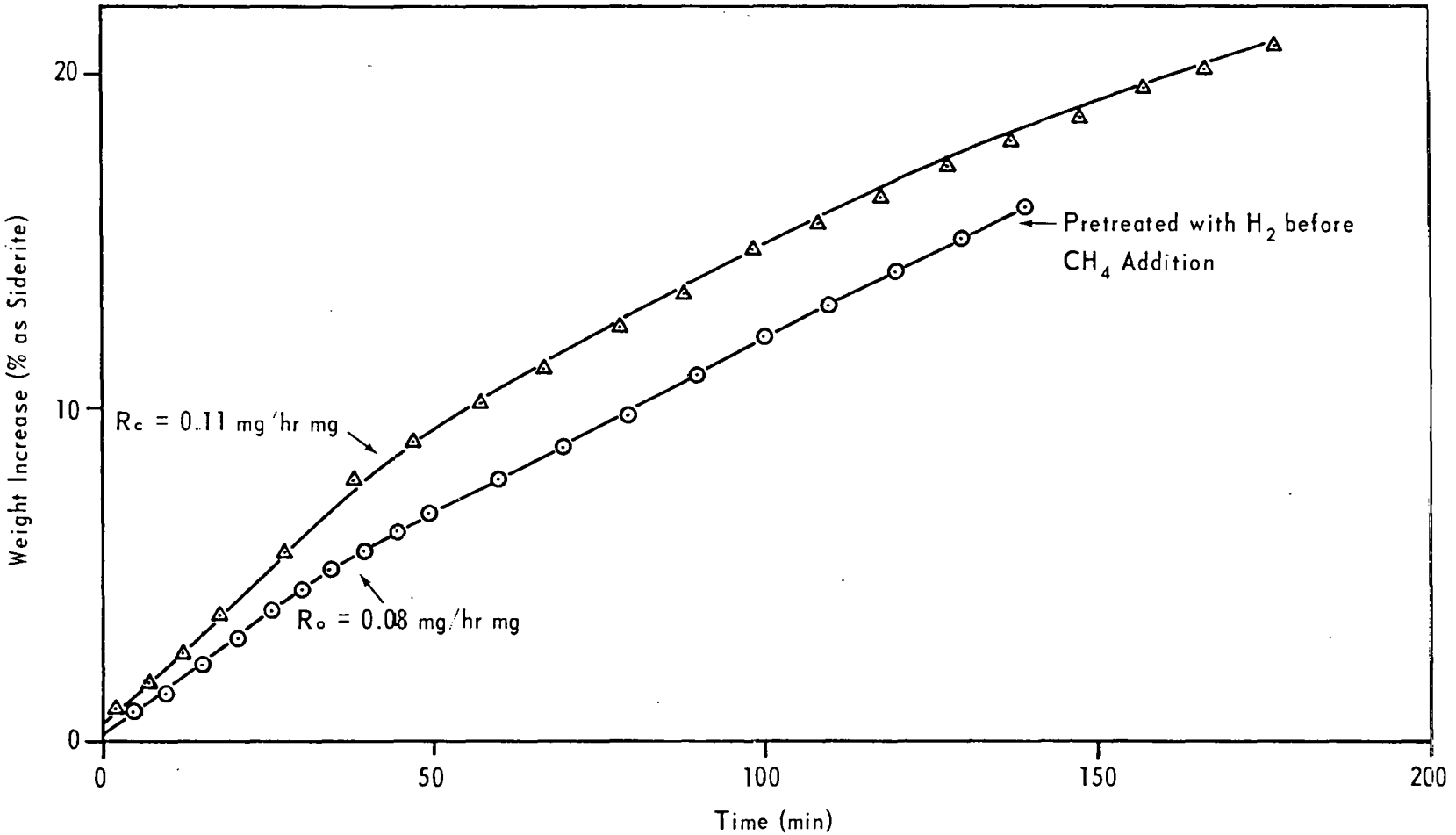

Figure 11 WEIGHT CHANGES OCCURRING DURING CRACKING OF METHANE ON SIDERITE AT 900° C

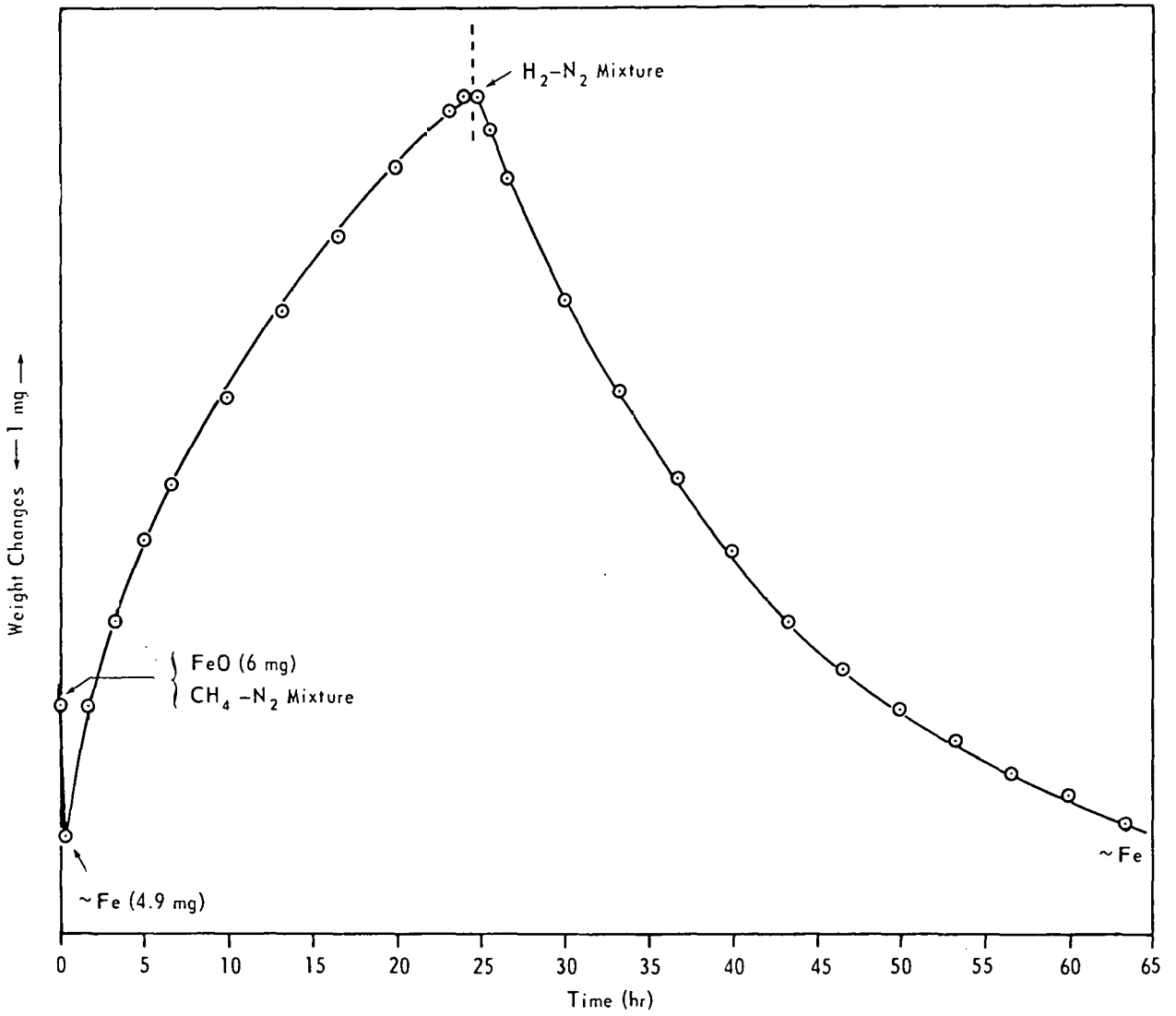

Figure 12 WEIGHT CHANGES OCCURRING DURING METHANE CRACKING ON SIDERITE AND SUBSEQUENT GASIFICATION IN HYDROGEN AT 900°C

It is known that treatment of FeO with hydrogen at 900°C results in the quantitative reduction of FeO to elemental iron. Following the reduction step, when the nitrogen-hydrogen mixture was replaced by the methane-nitrogen mixture, an increase in weight was observed, the maximum 'reaction' rate being 0.08 mg hr^{-1} mg^{-1}.

Since a platinum pan was used to contain siderite during heat treatment and subsequent reaction with methane, it may be argued that the platinum pan might have catalyzed the cracking of methane. In order to see if this were true, a quartz pan was used instead of the platinum pan to contain siderite. It was observed that the extent and rate of methane cracking were the same whether siderite was contained in a quartz or a platinum pan.

Iron derived from siderite catalyzes the cracking of methane for an extended period of time. Even after 23 hr the reaction does not tend to stop. The total weight increase in 23 hr is 170 percent the amount of iron contained in the starting weight of siderite. This weight increase can be due to carbon deposition and/or formation of iron carbide. It can be shown by simple calculations that the total weight increase is not due solely to the formation of iron carbide. Instead, the results indicate that a major proportion of the weight increase is due to carbon deposition. It is noteworthy that when after 23 hr the nitrogen-methane mixture is replaced by the hydrogen-nitrogen mixture, deposited carbon and iron carbide (if formed) react readily with hydrogen, as is seen in Figure 12.

At 800°C, methane reacted with FeO (derived from siderite) to the extent that after a weight loss amounting to about 30 percent of the starting weight of FeO the reaction stopped. However, if at 800°C methane was replaced by nitrogen and the system heated in nitrogen from 800 to 900°C, and at 900°C nitrogen was replaced by the methane-nitrogen mixture, significant cracking of methane, as indicated by a weight increase, was observed. The maximum rate of weight increase was 0.11 mg hr^{-1} mg^{-1} starting weight of siderite. This rate is the same if as shown earlier siderite is heated from ambient to 900°C in nitrogen and subsequently reacted with methane at this temperature.

Upon heating in a nitrogen atmosphere, calcite loses carbon dioxide in the temperature range 500-750°C. At 900°C when nitrogen was replaced by the nitrogen-methane mixture, a weight increase was observed; the slight weight increase continued monotonically with time. In the TGA run, the weight increase in 3 hr corresponded to about 3 percent of the starting weight of calcite. However, when the reaction was carried out in a tube furnace for an extended period of time, the corresponding weight increase in 15 hr was 10.6 percent.

When pyrite is heated in nitrogen up to 900°C, it loses some sulfur in the temperature range 280-700°C forming probably pyrrhotite(s). The resultant product was found not to catalyze the cracking of methane. However, when pyrite was reduced with hydrogen at 900°C, the resultant iron formed was an excellent catalyst for methane cracking.

This study was conducted because of our previous finding that carbon deposited from the cracking of hydrocarbons (of the type present in the volatile matter of coal) onto char surfaces subsequently reduced char

gasification rates. We wanted to examine the catalytic activity of various minerals found in coal. This study has shown that most minerals are inactive as catalysts for methane cracking. Thus, this study will be discontinued and reported in publication form.

REACTIVITY OF ION-EXCHANGED LIGNITE CHARS IN STEAM

Introduction

Reactivities in steam (650°C) have been measured for a series of chars prepared from a raw, demineralized and cation-exchanged Texas lignite. In addition, two coal chars have been demineralized, oxidized with nitric acid, and ion-exchanged prior to reactivity measurement. The major variables under investigation are concentration of exchanged cation, type of cation, conditions of exchange, and heat treatment temperature. All samples produced in this study have been characterized by a combination of ash measurement and ash content, densities in mercury and helium, particle size distributions, and surface area.

Experimental

A series of chars (700, 800, 900°C) has been prepared from raw, demineralized and calcium-exchanged (1.2 m moles cation/g coal) Darco, Texas lignite. Chars heated to 800°C were prepared from the demineralized coal exchanged to 10 different calcium exchange loadings (0.10 to 2.1 m moles/g) and from various cations (Na^{+1}, K^{+1}, Fe^{+3}, Ca^{+2}, and Mg^{+2}) exchanged to 0.3 m mole/g coal. Reactivities in steam (650°C) have been determined for all these chars by use of a fluidized bed reactor. To examine the effect of exchanged cations on the reactivity of a thermally stable structure, two raw coal chars (800 to 900°C) were demineralized, oxidized with nitric acid, ion-exchanged (Ca^{+2}, Fe^{+3}, Na^{+1}, and Mg^{+2}) and subsequently reheated.

In addition to the reactivity measurements, the coals and chars have been characterized by a combination of proximate analyses, densities in helium and mercury, size distributions, and carbon dioxide surface areas.

Since this study is near to completion, this quarter's work has been mainly concerned with data evaluation and consolidation. However, some x-ray diffraction profiles have been determined for selected samples of partially reacted, ion-exchanged chars. Partially reacted chars were selected because the relative concentrations of inorganic material are sufficient to allow x-ray determination of the major constituents without having to 'low temperature ash' the carbonaceous solid. For a highly calcium-loaded char, reacted to 45 percent burn-off, the major inorganic phase appeared to be calcite ($CaCO_3$). For a char derived from magnesium and iron exchange, the major constituents appear to be oxide forms of these elements. However, for the sodium and potassium-containing coal chars, it was very difficult to determine major phases. There are indications, from the x-ray data, that these chars contain a wide range of sulfate, sulfites, sulfides, and carbonates.

Results indicate: 1) that for a series of chars prepared from calcium-exchanged coals, there is a direct relationship between reactivity and amount of cation exchanged, 2) for chars prepared from coals containing equal amounts of various cations (K^{+1}, Na^{+1}, Ca^{+2}, Mg^{+2}, and Fe^{+3}), the most reactive chars are those derived from potassium, sodium and calcium. Magnesium is a poor catalyst. 3) Although iron containing chars are highly reactive in the initial stages of gasification in steam, their reactivity rapidly diminishes with time, which suggests a marked change in catalytic activity as the reaction proceeds.

COMBUSTION OF CHAR AND ANTHRACITE COAL IN LARGE UTILITY BOILERS

Introduction

Work has continued to be focused on the development of computer models to analyze and explain past experiments and to design future ones. A model of a pulverized char flame with an infinite parallel plane geometry was presented in a previous quarterly report.

The study of the infinite parallel plane model has provided insight into the effects of two major variables: fuel reactivity and combustor length.

The question of how important an influence furnace bottom temperature has on plane-flame furnace performance has been answered by comparing furnace performance for hot and cold bottom conditions. Also, in addition to the Exxon Illinois and Wyodak chars, and the FMC COED char, a fourth char has been burned in the plane-flame furnace at the same prescribed total air flow rate values.

Experimental

An experimental study was performed to determine the influence the furnace bottom temperature has on the combustion performance of fuels in the plane-flame furnace. The combustion chamber of the furnace is illustrated in Figure 13, with the bottom block's location with respect to the rest of the combustion chamber shown to scale. The cross section of the combustion chamber is 16.5 by 16.5 cm and the distance from the bottom of the water-cooled tube bank to the top surface of the bottom block is 170 cm. The actual procedure followed in this study was to first stabilize a coal char flame in the plane-flame furnace with the water-cooled cottom block in place, and then to replace the water-cooled bottom block by an uncooled refractory block while the char combustion continued. The char flame was then allowed to stabilize with the refractory block in place. Thus, two steady wall temperature profiles were obtained, one for the water cooled bottom and one for the refractory bottom.

The design of the water-cooled bottom block is shown in Figures 14 (top view) and 15 (front view). All components of the block are metal and all joints are soldered. The main body of the block is hollow, with two water inlets delivering cold water to the back of the block. The water then flows back through the body of the block and out the two water outlets provided. In actual operation, the water flow rate was so large as to completely rule out any rise in water temperature above ambient (15°C). Along one side of the block's surface, an air manifold is located to continuously distribute air to a series of holes drilled parallel to the top surface. The air jets issuing from these holes keep the top surface of the block free from ash deposit buildup under firing conditions.

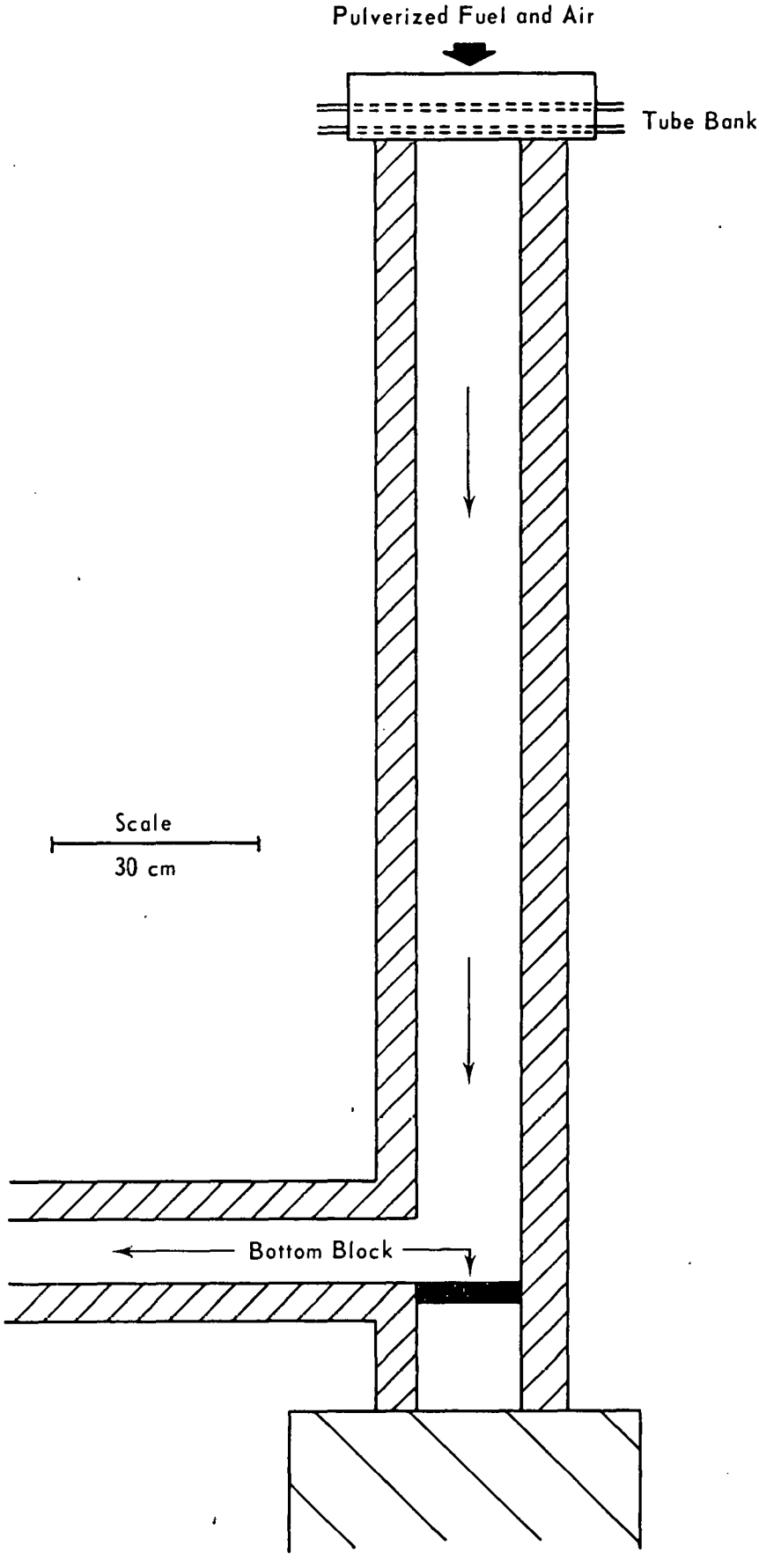

Figure 13 PLANE FLAME FURNACE WITH BOTTOM BLOCK

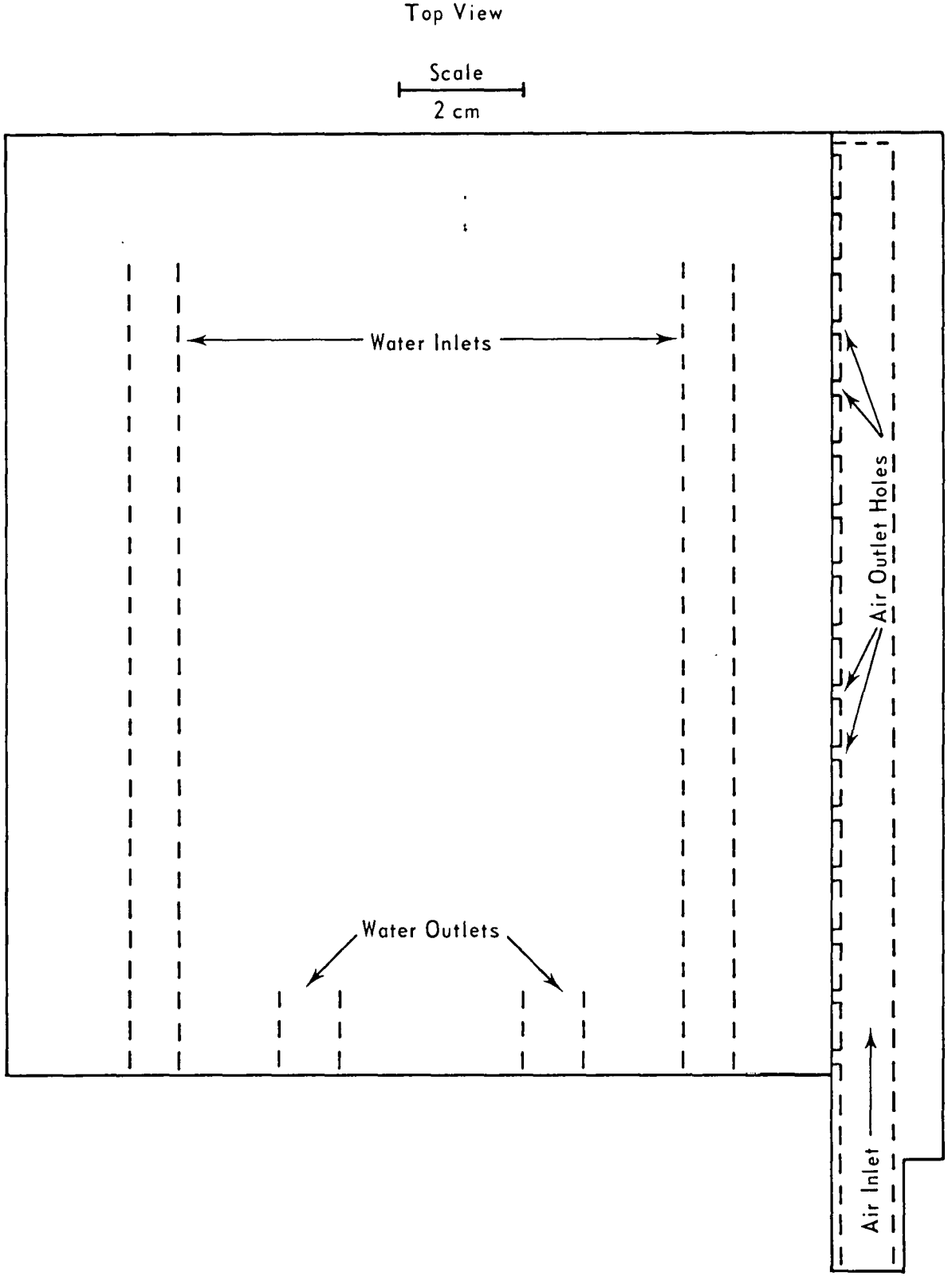

Figure 14 WATERCOOLED BOTTOM BLOCK

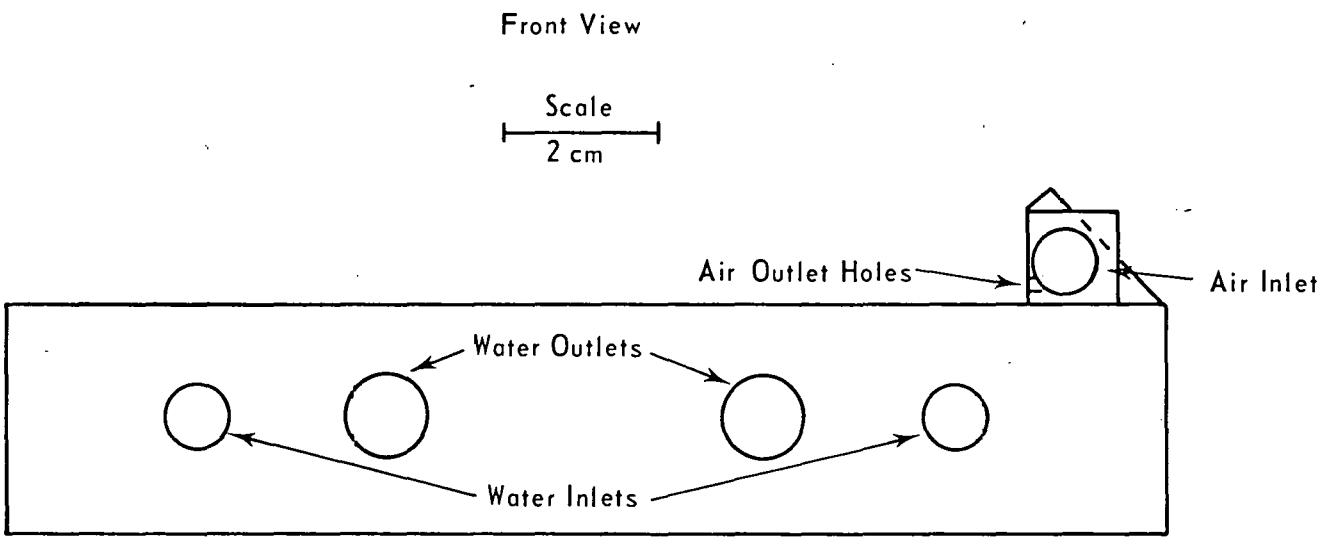

Figure 15 WATERCOOLED BOTTOM BLOCK

The refractory block is shown in Figures 16 (top view) and 17 (front view). The block was fabricated out of insulating brick, with the surface sealed with a furnace sealing paint to protect the surfaces and to prevent the air supplied to the delivery manifold from leaking out through the very porous brick. This block has no incorporated cooling mechanism, but the air jets parallel to the surface were used to make all the operating conditions except surface temperature identical for the two different bottom blocks.

The steady state wall temperature profiles for the water-cooled and the refractory bottoms are plotted in Figure 18. Near the tube bank, the water-cooled bottom wall temperatures are higher than the refractory bottom ones. The profiles cross at about 18 cm from the tube bank, and from there to about 100 cm from the tube bank the refractory bottom wall temperatures are consistently higher. The maximum difference in wall temperatures seems to occur around 60 cm, with the magnitude being 200°. The refractory bottom profile peaks out at 85 cm (1315°C) and declines slowly as the bottom is approached. On the other hand, the water-cooled profile peaks around 110 cm (1290°C) and drops sharply near the bottom. The main features to note are that the water-cooled bottom seems to shift the main body of the char flame roughly 8 to 10 cm toward the chamber exit, peak temperature is only affected by 25° and the temperatures in the tail of the flame are significantly influenced by the temperature of the furnace bottom.

A second experimental study conducted involved the burning of another coal char, referred to here as char No. 4, in the plane-flame furnace at the same standard total air flow rates as the two Exxon chars and the FMC COED char. The char under consideration was found to have the following proximate analysis: FC (fixed carbon) 69.75 percent, VM (volatile matter) 7.10 percent, and ASH 23.15 percent. Using a calculated LHV (lower heating value) of 10,861 Btu/lb, the required total net heat input of 100,000 Btu/hr was obtained with a pulverized char feed rate of 9.22 lb/hr.

In Figure 19, the wall temperature profiles for total air flow rate condition A (8.76 SCFM) are plotted for char No. 4, FMC COED char and the Exxon Wyodak char. It can easily be seen that the Exxon Wyodak wall temperature profile is quite different in general appearance from the char No. 4 and FMC COED char profiles. The latter two profiles are similar to each other, are shifted quite far downstream relative to the Exxon Wyodak profile, and have an 18 cm difference in flame front position between them. The profiles for condition B (11.55 SCFM) are plotted in Figure 20 and one again observes that the Exxon Wyodak profile is considerably different from the other two. Here, the char No. 4 wall temperatures are higher than the COED values for more than half of the combustion chamber length and the difference between flame front positions is only 10 cm, while it was about 18 cm for condition A. For condition C, the FMC COED was not able to be stabilized in the chamber. It should be noted that char No. 4 was able to be stabilized for condition C, while the COED char could not. For this condition, the maximum wall temperature point for char No. 4 is nearly at the end of the chamber, as is the corresponding visual flame front. Such observed behavior indicates further increases in total air flow rate will likely cause extinction. The Exxon Wyodak profile also shows the same tendency but to a lesser extent. When condition D was attempted, char No. 4 could not be stabilized and the flame was extinguished gradually with time. Our previous work[16] shows that the Exxon Wyodak char could easily be stabilized at condition D, the highest air flow used.

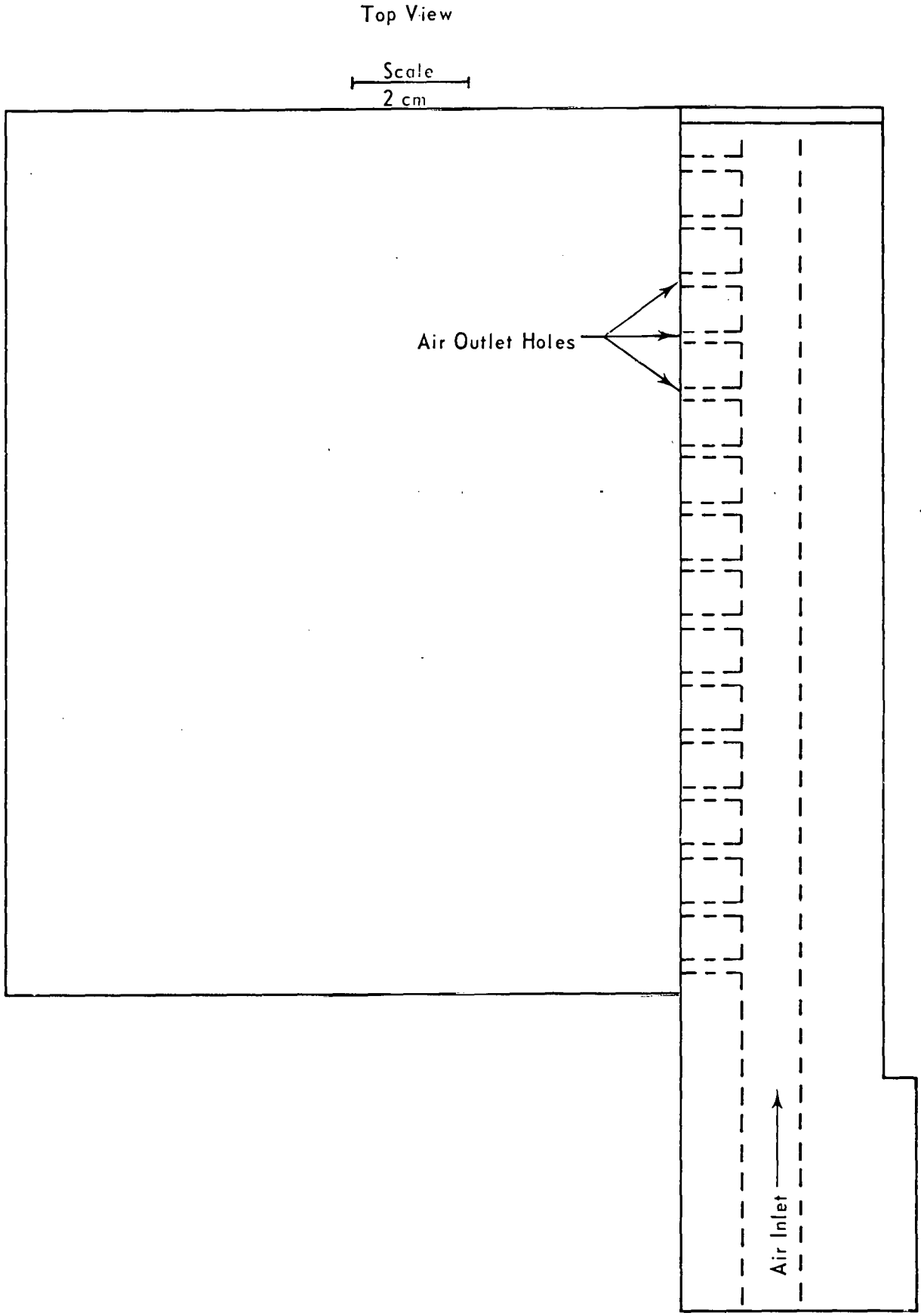

Figure 16 REFRACTORY BOTTOM BLOCK

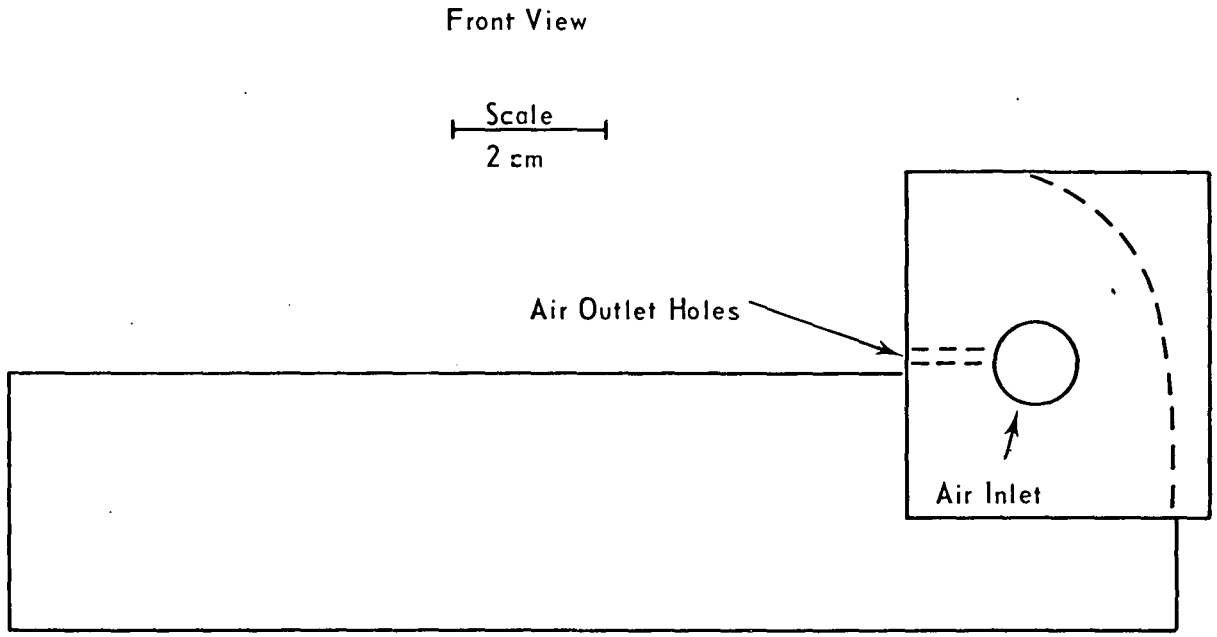

Figure 17 REFRACTORY BOTTOM BLOCK

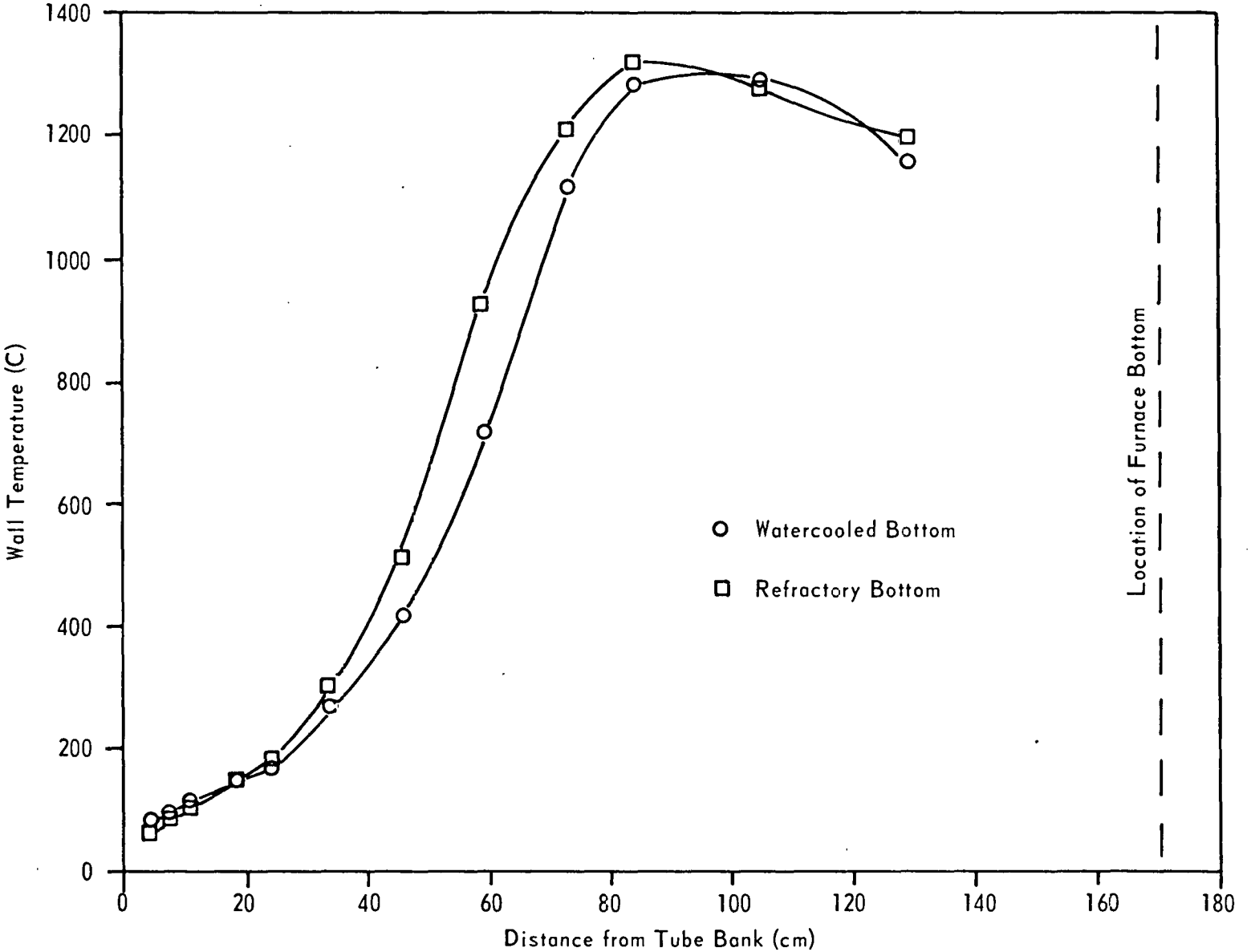

Figure 18 WALL TEMPERATURE PROFILES FOR PLANE FLAME FURNACE RUNS USING WATERCOOLED AND REFRACTORY BOTTOMS

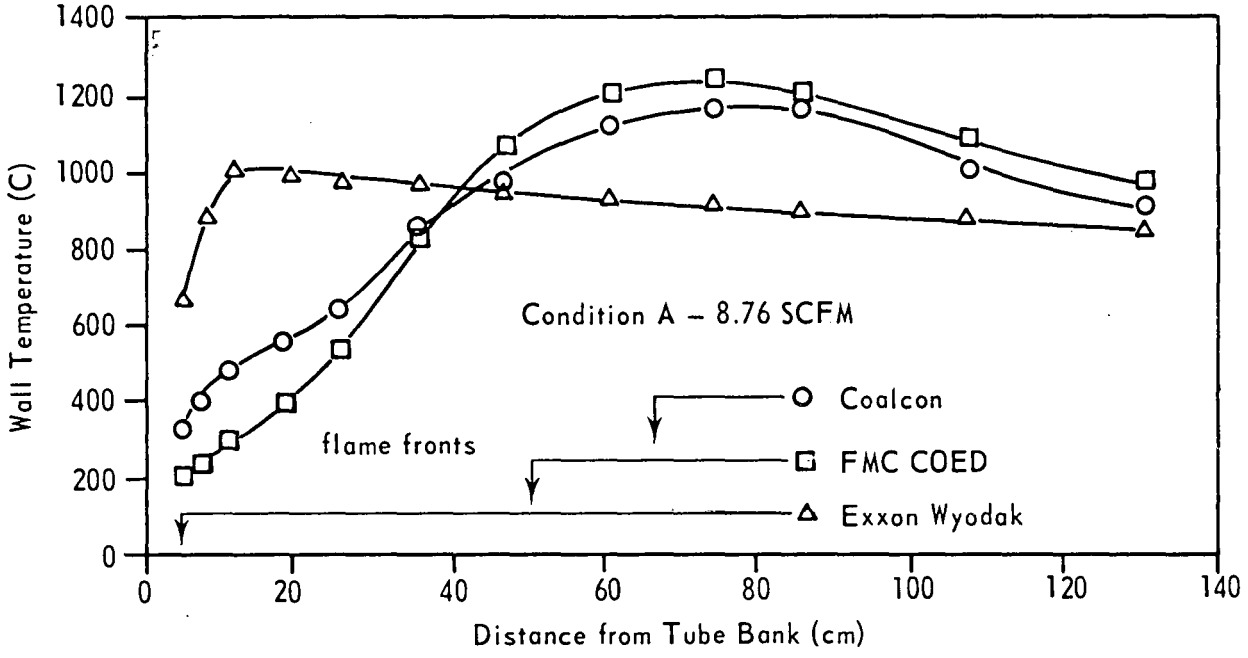

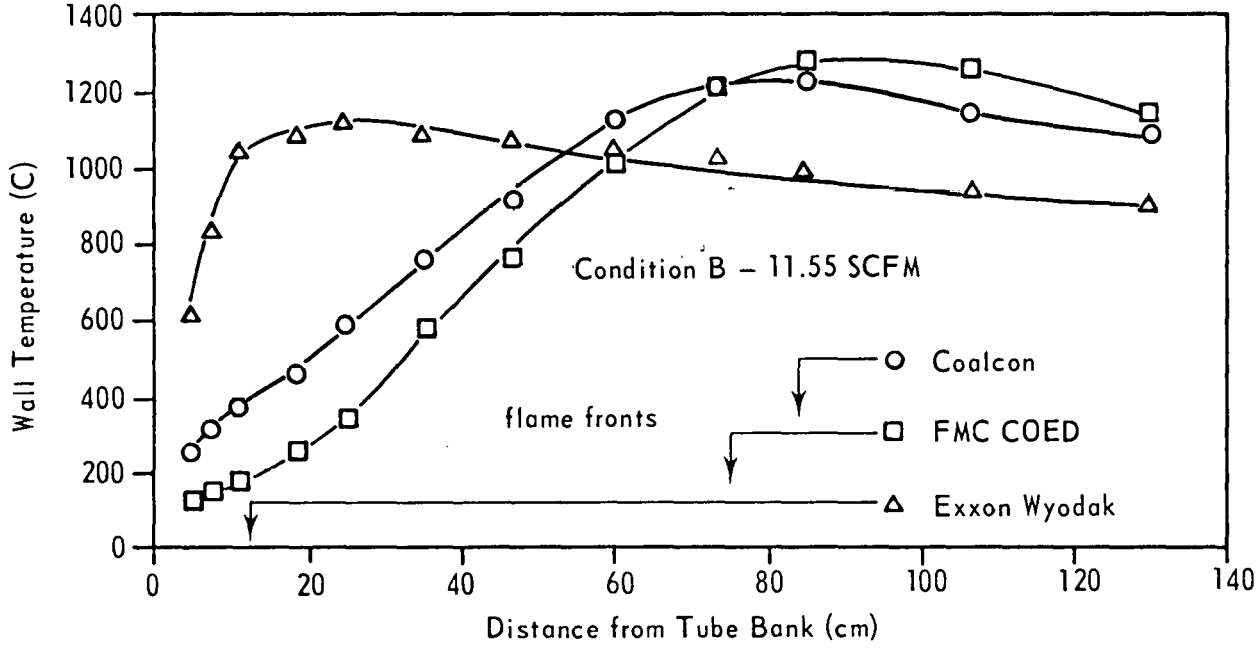

Figure 19 WALL TEMPERATURE PROFILES FOR CONDITIONS A AND B

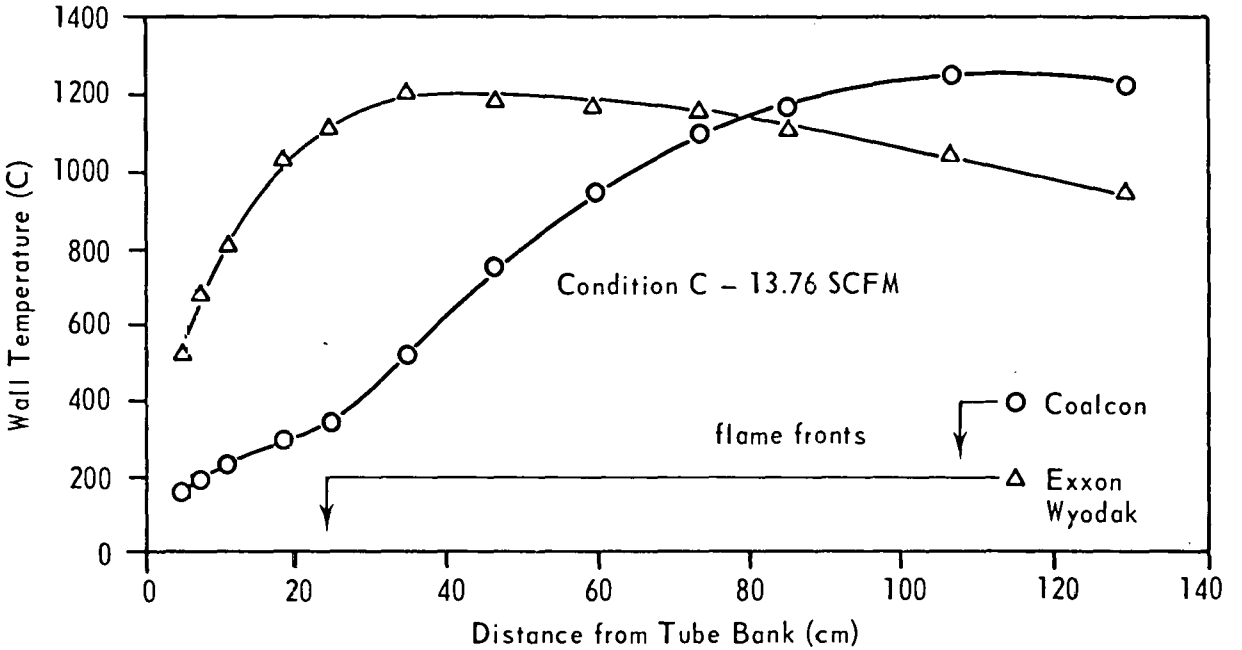

Figure 20 WALL TEMPERATURE PROFILES FOR CONDITION C

FACET V-B: COMBUSTION OF COAL-OIL EMULSIONS

COMBUSTION OF COAL-OIL-WATER MIXTURE

Introduction

During the past quarter investigation of the heat transfer characteristics of coal-oil-water-air mixtures continued, with an emphasis placed on attaining higher levels of coal addition. To characterize the hot-wall furnace described in previous reports, separate tests were run to assess the furnace thermal output as a function of firing rate.

Experimental

In departure from previous experiments, the starting coal-oil dispersions are now being prepared in the Combustion Laboratory. They consist of 50 percent by weight No. 6 fuel oil and 50 percent by weight coal sized under 106 μ. With the addition of small amounts of surfactant, the materials are mixed in a ball mill to be fed into the emulsifier through a gear pump. A significant amount of time and effort was spent in devising a pump system capable of handling the larger coal additions. Coal additions of 4.3 percent, 5.8 percent, and 7.2 percent have now been run, and the results have been consistent with previous results for lower levels of coal addition.

An important factor affecting these experiments is the influence of the firing rate on the thermal output and thermal efficiency of the furnace. After the initial 6 hr preheat period, No. 2 fuel oil was burned at a succession of increasing firing rates for specific durations, followed by a succession of deceasing firing rates. The same procedure was repeated for 4 consecutive days to reveal the effects of furnace dynamics. For each day the history of heat transfer versus firing rate revealed a narrow hysteresis loop. On successive days the hysteresis became less significant, with the most evident reduction occurring after one day. This suggests that an adequate furnace preheat period (of one day) should precede future experimental runs.

CONCLUSIONS

1. A cold model of the flow of gases through the combustion pot was constructed. Flow analyses indicate that even with relatively slow flows the mainstream flow is turbulent.

2. The weight mean size ($\bar{x}$) of char particles produced by pyrolysis of a given size grade of coal can be determined to a good accuracy (± 1 μm) at 95 percent confidence limits.

3. The methanol and water densities of a series of thirteen char samples have been found to be very close to each other as well as to the helium densities. The water and methanol densities both show a drift with time, but constant values are obtained within four and three days, respectively.

4. The maximum amount of carbon deposited from the cracking of methane on the surface of a lignite char is much less than the amount of total open pore volume which is potentially available to accommodate carbon. Carbon deposition reduces surface area and open pore volume of the char. Extensive subsequent gasification of the carbon deposition raw char does not open porosity to the extent that is found for gasification of the raw char. Deposition of carbon on the char reduces the diffusion parameter whereas gasification of the raw as well as carbon deposition chars increases the diffusion parameter.

5. For a Saran char associated with 18-22 ppm iron as an impurity, the heat of chemisorption of oxygen, ΔH, at 100°C is 38 ± 2 kcal/mole. For the oxygen-activated Saran, ΔH is 70 ± 2 kcal/mole at 75, 100, and 125°C. Both of these ΔH values are independent up to 28 min of reaction time. The unactivated and activated samples undergo gasification above 100 and 125°C, respectively. For the activated sample, significant physical adsorption takes place at 75°C.

6. Siderite and calcite catalyze the cracking of methane at 900°C; the catalytic activity is much more pronounced for siderite. The cracking of methane on siderite occurs for extended periods of time. After about 24 hr reaction time, the weight increase is about 170 percent the weight of iron contained in the starting weight of siderite. The major proportion of the weight increase has been attributed to carbon deposition. The pronounced catalytic activity for methane cracking is thought to be due to the formation of elemental iron. Dolomite, pyrite, illite, quartz, rutile, and kaolinite have no catalytic activity for methane cracking. Gypsum 'reacts' with methane but there is no indication of carbon deposition.

7. It has been shown that large amounts of inorganic materials can be added to lignite by ion exchange. This exchange can result in marked increases in reactivity of subsequent chars in steam. It appears as though different cations lead to different catalytic properties in chars. In the case of calcium, it has been shown that there is a direct relationship between reactivity and amount of calcium present (within the range studied). Char prepared from K^{+1} is more reactive than those derived from other cations. Exchanged magnesium leads to a remarkably low reactivity. In the case of iron, it appears that the catalytic species derived from the iron ions undergoes a marked change during reaction with steam, since the reactivity of these chars decreases as reaction proceeds.

8. From a comparison of refractory and water-cooled bottom blocks it can be concluded that even significant changes in the furnace bottom temperature can only cause moderate changes in plane-flame furnace combustion performance. Since the char used for this study stabilized quite far down from the tube bank (in comparison to the Exxon chars), the results of this study establish the maximum effect that the furnace bottom temperature can have on combustion performance. The study involving the burning of char No. 4 is interpreted as meaning that char No. 4 is more reactive than the FMC COED char, but still quite less reactive than the two Exxon chars. These results are the first such set where a fuel whose flame front is closer to the tube bank than that of a second fuel actually has initial wall temperatures lower than those of the second fuel.

9. Coal in amounts up to 7 percent have been added to oil-water-air emulsions to determine combustion characteristics. The heat output from the hot wall test furnace has been observed to increase with increasing coal additions, without significant changes in excess air requirements for complete combustion.

   Separate tests have revealed a changing hysteresis effect in the thermal output of the furnace as a function of firing rate, suggesting that adequate preheat periods should be provided before subsequent test runs.

REFERENCES

1. Ondrick, C.W., and G.S. Srivastava. Corfan-Fortran IV Computer Program for Correlation, Factor Analysis (R- and Q-Mode) and Varimax Rotation. Kansas State Geological Survey, Computer Contribution 42, 92 pp.

2. Spackman, W., A. Davis, P.L. Walker, H.L. Lovell, R.H. Essenhigh, F.J. Vastola, and P.H. Given. The Characteristics of American Coals in Relation to Their Conversion into Clean Energy Fuels. Qtr. Tech. Prog. Rept to ERDA for the Period April-June 1976, 72 pp.

3. Carman, P.C. Trans. Inst. Chem. Engrs. (London), v. 15, p. 150, 1937.

4. Field, M.A., D.W. Gill, B.B. Morgan, and P.G.W. Hawksley. Combustion of Pulverized Coal. BCURA, Leatherhead, England, p. 245, 1967.

5. Dean, R.B., and W.J. Dixon. Simplified Statistics for Small Numbers of Observations. Analytical Chemistry, v. 23, p. 636, 1951.

6. The Efficient Use of Fuel, 3rd ed. Her Majesty's Stationary Office, London, p. 109, 1969.

7. Gan, H., S.P. Nandi, and P.L. Walker, Jr. Nature of the Porosity in American Coals. Fuel, v. 51, p. 272, 1972.

8. Walker, Jr., P.L., R.C. Bansal, and F.J. Vastola. Studies on Ultra-Clean Carbon Surfaces I. Characterization of Surface Activity of Graphon by Room-Temperature Oxygen Chemisorption, in The Structure and Chemistry of Solid Surfaces, John Wiley and Sons, Inc., New York, p. 81-1, 1969.

9. Puri, B.R. Surface Complexes of Carbon, in Chemistry and Physics of Carbon, Marcel Dekker, New York, v. 6, p. 191, 1970.

10. Nelson, E.T., and P.L. Walker, Jr. Some Techniques for Investigating the Unsteady-State Molecular Flow of Gas Through a Microporous Medium. J. Appl. Chem., v. 11, p. 358, 1961.

11. Nandi, S.P., and P.L. Walker, Jr. Activated Diffusion of Methane from Coals at Elevated Pressures. Fuel, v. 54, p. 81, 1975.

12. _____ The Diffusion of Nitrogen and Carbon Dioxide from Coals of Various Rank. Fuel, v. 43, p. 385, 1964.

13. Lamond, T.G., and H. Marsh. The Surface Properties of Carbon. II. The Effect of Capillary Condensation of Low Reactive Pressures Upon the Determination of Surface Area. Carbon, v. 1, p. 281, 1964.

14. Walker, Jr., P.L., L.G. Austin, and S.P. Nandi. Activated Diffusion of Gases in Molecular Sieve Materials, in Chemistry and Physics of Carbon, Marcel Dekker, New York, v. 2, p. 257, 1966.

15. Walker, Jr., P.L., F.J. Rusinko, and L.G. Austin. Gas Reactions of Carbons, in Advances in Catalysis, Academic Press, New York, v. 11, p. 133, 1959.

16. Essenhigh, R.H., and J.G. Cogoli. Pulverized Char Combustion in a Laboratory Scale Furnace. 170th National Meeting ACS, Division of Fuel Chemistry, v. 20, no. 3, p. 134, 1975.

The following individuals have made contributions to this report:

J.C. Cogoli, C.P. Dolsen, T. Eapen, J. Friehaut, E. Gootzait, E.J. Hippo, D.S. Hoover, J.M. Hower, I.K. Ismail, R.G. Jenkins, M. Kamishita, A. Kokkinos, K.W. Kuehn, A.A. Leff, A. Linares, O.P. Mahajan, N. Nsakala, H.E. Shull, C.T. Waddell, and A. Youssef.

☆ U.S. GOVERNMENT PRINTING OFFICE: 1977-740-094/163